
Is Heterophily A Real Nightmare For Graph Neural Networks To Do Node Classification?

Sitao Luan^{1,2}, Chenqing Hua¹, Qincheng Lu¹, Jiaqi Zhu¹, Mingde Zhao^{1,2}, Shuyuan Zhang^{1,2},
Xiao-Wen Chang¹, Doina Precup^{1,2,3}

{sitao.luan@mail, chenqing.hua@mail, qincheng.lu@mail, jiaqi.zhu@mail, mingde.zhao@mail,
shuyuan.zhang@mail, chang@cs, dprecup@cs}.mcgill.ca

¹McGill University; ²Mila; ³DeepMind

Abstract

Graph Neural Networks (GNNs) extend basic Neural Networks (NNs) by using the graph structures based on the relational inductive bias (homophily assumption). Though GNNs are believed to outperform NNs in real-world tasks, performance advantages of GNNs over graph-agnostic NNs seem not generally satisfactory. Heterophily has been considered as a main cause and numerous works have been put forward to address it. In this paper, we first show that not all cases of heterophily are harmful ¹ for GNNs with aggregation operation. Then, we propose new metrics based on a similarity matrix which considers the influence of both graph structure and input features on GNNs. The metrics demonstrate advantages over the commonly used homophily metrics by tests on synthetic graphs. From the metrics and the observations, we find some cases of harmful heterophily can be addressed by diversification operation. With this fact and knowledge of filterbanks, we propose the Adaptive Channel Mixing (ACM) framework to adaptively exploit aggregation, diversification and identity channels in each GNN layer to address harmful heterophily. We validate the ACM-augmented baselines with 10 real-world node classification tasks. They consistently achieve significant performance gain and exceed the state-of-the-art GNNs on most of the tasks without incurring significant computational burden.

1 Introduction

Deep Neural Networks (NNs) [21] have revolutionized many machine learning areas, including image recognition [20], speech recognition [13] and natural language processing [2], *etc.* One major strength is their capacity and effectiveness of learning latent representation from Euclidean data. Recently, the focus has been put on its applications on non-Euclidean data [5], *e.g.*, relational data or graphs. Combining graph signal processing and convolutional neural networks [22], numerous Graph Neural Networks (GNNs) [34, 9, 15, 35, 18, 28] have been proposed which empirically outperform traditional neural networks on graph-based machine learning tasks, *e.g.*, node classification, graph classification, link prediction and graph generation, *etc.* GNNs are built on the homophily assumption [31], *i.e.*, connected nodes tend to share similar attributes with each other [14], which offers additional information besides node features. Such relational inductive bias [3] is believed to be a key factor leading to GNNs' superior performance over NNs' in many tasks.

Nevertheless, growing evidence shows that GNNs do not always gain advantages over traditional NNs when dealing with relational data. In some cases, even simple Multi-Layer Perceptrons (MLPs) can outperform GNNs by a large margin [40, 26, 7]. An important reason for the performance degradation

¹In general, harmful heterophily means the heterophilous structure that will make a graph-aware model underperform its corresponding graph-agnostic model.

is believed to be the heterophily problem, *i.e.*, connected nodes tend to have different labels which makes the homophily assumption fail. Heterophily challenge has received attention recently and there are increasing number of models being put forward to address this problem [40, 26, 7, 39, 38].

Contributions In this paper, we first demonstrate that not all heterophilous graphs are harmful for aggregation-based GNNs and the existing metrics of homophily are insufficient to decide whether the aggregation operation will make nodes less distinguishable or not. By constructing a similarity matrix from backpropagation analysis, we derive new metrics to depict how much GNNs are influenced by the graph structure and node features. We show the advantage of our metrics over the existing metrics by comparing the ability of characterizing the performance of two baseline GNNs on synthetic graphs of different levels of homophily. From the similarity matrix, we find that diversification operation is able to address some harmful heterophily cases, and based on which we propose Adaptive Channel Mixing (ACM) GNN framework. The experiments on the synthetic datasets, ablation studies and real-world datasets consistently show that the baseline GNNs augmented by ACM framework are able to obtain significant performance boost on node classification tasks on heterophilous graphs.

The rest of this paper is mainly organized as follows: In section 2, we introduce the notation and the background knowledge. In section 3, we conduct node-wise analysis on heterophily, derive new homophily metrics based on a similarity matrix and conduct experiments to show their advantages over the existing homophily metrics. In section 4, we demonstrate the capability of diversification operation on addressing some cases of harmful heterophily and propose the ACM-GNN framework to adaptively utilize the information from different filterbank channels to address heterophily problem. In section 5, we discuss the related works and clarify the differences to our method. In section 6, we provide empirical evaluations on ACM framework, including ablation study and tests on 10 real-world node classification tasks.

2 Preliminaries

We will introduce the related notation and background knowledge in this section. We use **bold** fonts for vectors (*e.g.*, \mathbf{v}). Suppose we have an undirected connected graph $\mathcal{G} = (\mathcal{V}, \mathcal{E}, A)$, where \mathcal{V} is the node set with $|\mathcal{V}| = N$; \mathcal{E} is the edge set without self-loop; $A \in \mathbb{R}^{N \times N}$ is the symmetric adjacency matrix with $A_{i,j} = 1$ iff $e_{ij} \in \mathcal{E}$, otherwise $A_{i,j} = 0$. We use D to denote the diagonal degree matrix of \mathcal{G} , *i.e.*, $D_{i,i} = d_i = \sum_j A_{i,j}$ and use \mathcal{N}_i to denote the neighborhood set of node i , *i.e.*, $\mathcal{N}_i = \{j : e_{ij} \in \mathcal{E}\}$. A graph signal is a vector $\mathbf{x} \in \mathbb{R}^N$ defined on \mathcal{V} , where x_i is defined on the node i . We also have a feature matrix $X \in \mathbb{R}^{N \times F}$, whose columns are graph signals and whose i -th row $X_{i,:}$ is a feature vector of node i . We use $Z \in \mathbb{R}^{N \times C}$ to denote the label encoding matrix, whose i -th row $Z_{i,:}$ is the one-hot encoding of the label of node i .

2.1 Graph Laplacian, Affinity Matrix and Their Variants

The (combinatorial) graph Laplacian is defined as $L = D - A$, which is Symmetric Positive Semi-Definite (SPSD) [8]. Its eigendecomposition gives $L = U\Lambda U^T$, where the columns \mathbf{u}_i of $U \in \mathbb{R}^{N \times N}$ are orthonormal eigenvectors, namely the *graph Fourier basis*, $\Lambda = \text{diag}(\lambda_1, \dots, \lambda_N)$ with $\lambda_1 \leq \dots \leq \lambda_N$, and these eigenvalues are also called *frequencies*. The graph Fourier transform of the graph signal \mathbf{x} is defined as $\mathbf{x}_{\mathcal{F}} = U^{-1}\mathbf{x} = U^T\mathbf{x} = [\mathbf{u}_1^T\mathbf{x}, \dots, \mathbf{u}_N^T\mathbf{x}]^T$, where $\mathbf{u}_i^T\mathbf{x}$ is the component of \mathbf{x} in the direction of \mathbf{u}_i .

In addition to L , some variants are also commonly used, *e.g.*, the symmetric normalized Laplacian $L_{\text{sym}} = D^{-1/2}LD^{-1/2} = I - D^{-1/2}AD^{-1/2}$ and the random walk normalized Laplacian $L_{\text{rw}} = D^{-1}L = I - D^{-1}A$. The affinity (transition) matrices can be derived from the Laplacians, *e.g.*, $A_{\text{rw}} = I - L_{\text{rw}} = D^{-1}A$, $A_{\text{sym}} = I - L_{\text{sym}} = D^{-1/2}AD^{-1/2}$ and are considered to be low-pass filters [30]. Their eigenvalues satisfy $\lambda_i(A_{\text{rw}}) = \lambda_i(A_{\text{sym}}) = 1 - \lambda_i(L_{\text{sym}}) = 1 - \lambda_i(L_{\text{rw}}) \in (-1, 1]$. Applying the renormalization trick [18] to affinity and Laplacian matrices respectively leads to $\hat{A}_{\text{sym}} = \tilde{D}^{-1/2}\tilde{A}\tilde{D}^{-1/2}$ and $\hat{L}_{\text{sym}} = I - \hat{A}_{\text{sym}}$, where $\tilde{A} \equiv A + I$ and $\tilde{D} \equiv D + I$. The renormalized affinity matrix essentially adds a self-loop to each node in the graph, and is widely used in Graph Convolutional Network (GCN) [18] as follows,

$$Y = \text{softmax}(\hat{A}_{\text{sym}} \text{ReLU}(\hat{A}_{\text{sym}} X W_0) W_1) \quad (1)$$

where $W_0 \in \mathbb{R}^{F \times F_1}$ and $W_1 \in \mathbb{R}^{F_1 \times O}$ are learnable parameter matrices. GCN can be trained by minimizing the following cross entropy loss

$$\mathcal{L} = -\text{trace}(Z^T \log Y) \quad (2)$$

where $\log(\cdot)$ is a component-wise logarithm operation. The random walk renormalized matrix $\hat{A}_{\text{rw}} = \tilde{D}^{-1} \tilde{A}$, which shares the same eigenvalues as \hat{A}_{sym} , can also be applied in GCN. The corresponding Laplacian is defined as $\hat{L}_{\text{rw}} = I - \hat{A}_{\text{rw}}$. \hat{A}_{rw} is essentially a random walk matrix and behaves as a mean aggregator that is applied in spatial-based GNNs [15, 14]. To bridge the spectral and spatial methods, we use \hat{A}_{rw} in the paper.

2.2 Metrics of Homophily

The metrics of homophily are defined by considering different relations between node labels and graph structures defined by adjacency matrix. There are three commonly used homophily metrics: edge homophily [1, 40], node homophily [33], and class homophily [24]² defined as follows:

$$\begin{aligned} H_{\text{edge}}(\mathcal{G}) &= \frac{|\{e_{uv} \mid e_{uv} \in \mathcal{E}, Z_{u,:} = Z_{v,:}\}|}{|\mathcal{E}|}, & H_{\text{node}}(\mathcal{G}) &= \frac{1}{|\mathcal{V}|} \sum_{v \in \mathcal{V}} \frac{|\{u \mid u \in \mathcal{N}_v, Z_{u,:} = Z_{v,:}\}|}{d_v}, \\ H_{\text{class}}(\mathcal{G}) &= \frac{1}{C-1} \sum_{k=1}^C \left[h_k - \frac{|\{v \mid Z_{v,k} = 1\}|}{N} \right]_+, & h_k &= \frac{\sum_{v \in \mathcal{V}} |\{u \mid Z_{v,k} = 1, u \in \mathcal{N}_v, Z_{u,:} = Z_{v,:}\}|}{\sum_{v \in \{v \mid Z_{v,k} = 1\}} d_v} \end{aligned} \quad (3)$$

where $[a]_+ = \max(a, 0)$; h_k is the class-wise homophily metric [24]. They are all in the range of $[0, 1]$ and a value close to 1 corresponds to strong homophily while a value close to 0 indicates strong heterophily. $H_{\text{edge}}(\mathcal{G})$ measures the proportion of edges that connect two nodes in the same class; $H_{\text{node}}(\mathcal{G})$ evaluates the average proportion of edge-label consistency of all nodes; $H_{\text{class}}(\mathcal{G})$ tries to avoid the sensitivity to imbalanced class, which can cause H_{edge} misleadingly large. The above definitions are all based on the graph-label consistency and imply that the inconsistency will cause harmful effect to the performance of GNNs. With this in mind, we will show a counter example to illustrate the insufficiency of the above metrics and propose new metrics in the following section.

3 Analysis of Heterophily

3.1 Motivation and Aggregation Homophily

Heterophily is believed to be harmful for message-passing based GNNs [40, 33, 7] because intuitively features of nodes in different classes will be falsely mixed and this will lead nodes indistinguishable [40]. Nevertheless, it is not always the case, *e.g.*, the bipartite graph shown in Figure 1 is highly heterophilous according to the homophily metrics in (3), but after mean aggregation, the nodes in classes 1 and 2 only exchange colors and are still distinguishable. Authors in [7] also point out the insufficiency of H_{node} by examples to show that different graph typologies with the same H_{node} can carry different label information.

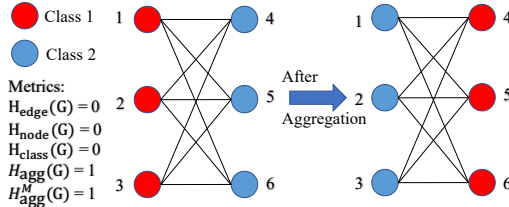


Figure 1: Example of harmless heterophily

To analyze to what extent the graph structure can affect the output of a GNN, we first simplify the GCN by removing its nonlinearity as [36]. Let $\hat{A} \in \mathbb{R}^{N \times N}$ denote a general aggregation operator. Then, equation (1) can be simplified as,

$$Y = \text{softmax}(\hat{A}XW) = \text{softmax}(Y') \quad (4)$$

²The authors in [24] did not name this homophily metric. We name it class homophily based on its definition.

After each gradient decent step $\Delta W = \gamma \frac{d\mathcal{L}}{dW}$, where γ is the learning rate, the update of Y' will be (see Appendix B for derivation),

$$\Delta Y' = \hat{A}X\Delta W = \gamma \hat{A}X \frac{d\mathcal{L}}{dW} \propto \hat{A}X \frac{d\mathcal{L}}{dW} = \hat{A}X X^T \hat{A}^T (Z - Y) = S(\hat{A}, X)(Z - Y) \quad (5)$$

where $S(\hat{A}, X) \equiv \hat{A}X(\hat{A}X)^T$ is a post-aggregation node similarity matrix, $Z - Y$ is the prediction error matrix. The update direction of node i is essentially a weighted sum of the prediction error, *i.e.*, $\Delta(Y')_{i,:} = \sum_{j \in \mathcal{V}} [S(\hat{A}, X)]_{i,j} (Z - Y)_{j,:}$.

To study the effect of heterophily, we first define the *aggregation similarity score* as follows.

Definition 1. *Aggregation similarity score*

$$S_{\text{agg}}(S(\hat{A}, X)) = \frac{\left| \left\{ v \mid \text{Mean}_u(\{S(\hat{A}, X)_{v,u} \mid Z_{u,:} = Z_{v,:}\}) \geq \text{Mean}_u(\{S(\hat{A}, X)_{v,u} \mid Z_{u,:} \neq Z_{v,:}\}) \right\} \right|}{|\mathcal{V}|} \quad (6)$$

where $\text{Mean}_u(\{\cdot\})$ takes the average over u of a given multiset of values or variables.

$S_{\text{agg}}(S(\hat{A}, X))$ measures the proportion of nodes $v \in \mathcal{V}$ that will put relatively larger similarity weights on nodes in the same class than in other classes after aggregation. It is easy to see that $S_{\text{agg}}(S(\hat{A}, X)) \in [0, 1]$. But in practice, we observe that in most datasets, we will have $S_{\text{agg}}(S(\hat{A}, X)) \geq 0.5$. Based on this observation, we rescale (6) to the following modified aggregation similarity for practical usage,

$$S_{\text{agg}}^M(S(\hat{A}, X)) = \left[2S_{\text{agg}}(S(\hat{A}, X)) - 1 \right]_+ \quad (7)$$

In order to measure the consistency between labels and graph structures without considering node features and make a fair comparison with the existing homophily metrics in (3), we define the graph (\mathcal{G}) aggregation (\hat{A}) homophily and its modified version as

$$H_{\text{agg}}(\mathcal{G}) = S_{\text{agg}}(S(\hat{A}, Z)), \quad H_{\text{agg}}^M(\mathcal{G}) = S_{\text{agg}}^M(S(\hat{A}, Z)) \quad (8)$$

In practice, we will only check $H_{\text{agg}}(\mathcal{G})$ when $H_{\text{agg}}^M(\mathcal{G}) = 0$. As Figure 1 shows, when $\hat{A} = \hat{A}_{\text{rw}}$, $H_{\text{agg}}(\mathcal{G}) = H_{\text{agg}}^M(\mathcal{G}) = 1$. Thus, this new metric reflects the fact that nodes in classes 1 and 2 are still highly distinguishable after aggregation, while other metrics mentioned before fail to capture the information and misleadingly give value 0. This shows the advantage of $H_{\text{agg}}(\mathcal{G})$ and $H_{\text{agg}}^M(\mathcal{G})$ by additionally considering information from aggregation operator \hat{A} and the similarity matrix.

To comprehensively compare $H_{\text{agg}}^M(\mathcal{G})$ with the metrics in (3) in terms of how they reveal the influence of graph structure on the GNN performance, we generate synthetic graphs and evaluate SGC [36] and GCN [18] on them in the next subsection.

3.2 Evaluation and Comparison on Synthetic Graphs

Data Generation & Experimental Setup We first generate 280 graphs in total with 28 edge homophily levels varied from 0.005 to 0.95, each corresponding to 10 graphs. For every generated graph, we have 5 classes with 400 nodes in each class. For each node, we randomly generate 2 intra-class edges and $\lfloor \frac{2}{h} - 2 \rfloor$ inter-class edges (see the details about the data generation process in appendix C). The features of nodes in each class are sampled from node features in the corresponding class of the base dataset. Nodes are randomly split into 60%/20%/20% for train/validation/test. We train 1-hop SGC (*sgc-1*) [36] and GCN [18] on synthetic data (see appendix A.1 for hyperparameter searching range). For each value of $H_{\text{edge}}(\mathcal{G})$, we take the average test accuracy and standard deviation of runs over 10 generated graphs. For each generated graph, we also calculate its $H_{\text{node}}(\mathcal{G})$, $H_{\text{class}}(\mathcal{G})$ and $H_{\text{agg}}^M(\mathcal{G})$. Model performance with respect to different homophily values are shown in Figure 2.

Comparison of Homophily Metrics The performance of SGC-1 and GCN are expected to be monotonically increasing with a proper and informative homophily metric. However, Figure 2(a)(b)(c)

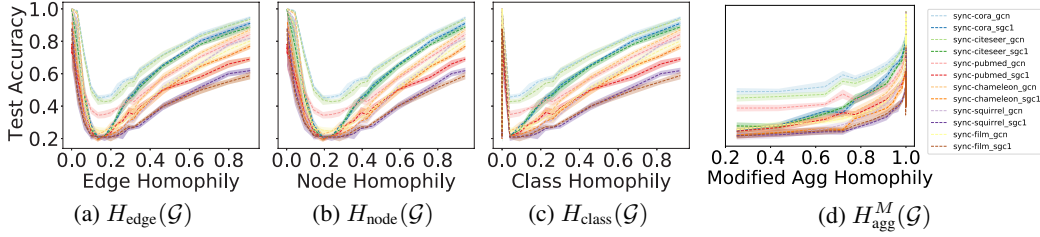


Figure 2: Comparison of baseline performance under different homophily metrics.

show that the performance curves under $H_{\text{edge}}(\mathcal{G})$, $H_{\text{node}}(\mathcal{G})$ and $H_{\text{class}}(\mathcal{G})$ are U -shaped³, while Figure 2(d) reveals a nearly monotonic curve with a little perturbation around 1. This indicates that $H_{\text{agg}}^M(\mathcal{G})$ can describe how the graph structure affects the performance of SGC-1 and GCN more appropriately and adequately than the existing metrics.

In addition, we notice that in Figure 2(a), both SGC-1 and GCN get the worst performance on all datasets when $H_{\text{edge}}(\mathcal{G})$ is around somewhere between 0.1 and 0.2. This interesting phenomenon can be explained by the following theorem based on the similarity matrix which can verify the usefulness of $H_{\text{agg}}^M(\mathcal{G})$.

Theorem 1. (See Appendix D for proof). Suppose there are C classes in the graph \mathcal{G} and \mathcal{G} is a d -regular graph (each node has d neighbors). Given d , edges for each node are *i.i.d.* generated, such that each edge of any node has probability h to connect with nodes in the same class and probability $1 - h$ to connect with nodes in different classes. Let the aggregation operator $\hat{A} = \hat{A}_{\text{rw}}$. Then, for nodes v , u_1 and u_2 , where $Z_{u_1,:} = Z_{v,:}$ and $Z_{u_2,:} \neq Z_{v,:}$, we have

$$g(h) \equiv \mathbb{E} \left(S(\hat{A}, Z)_{v,u_1} \right) - \mathbb{E} \left(S(\hat{A}, Z)_{v,u_2} \right) = \left(\frac{(C-1)(hd+1) - (1-h)d}{(C-1)(d+1)} \right)^2 \quad (9)$$

and the minimum of $g(h)$ is reached at

$$h = \frac{d+1-C}{Cd} = \frac{d_{\text{intra}}/h + 1 - C}{C(d_{\text{intra}}/h)} \Rightarrow h = \frac{d_{\text{intra}}}{Cd_{\text{intra}} + C - 1}$$

where $d_{\text{intra}} = dh$, which is the expected number of neighbors of a node that have the same label as the node.

The value of $g(h)$ in (9) is the expected differences of the similarity values between nodes in the same class as v and nodes in other classes. $g(h)$ is strongly related to the definition of aggregation homophily and its minimum potentially implies the worst value of $H_{\text{agg}}(\mathcal{G})$. In the synthetic experiments, we have $d_{\text{intra}} = 2$, $C = 5$ and the minimum of $g(h)$ is reached at $h = 1/7 \approx 0.14$, which corresponds to the lowest point in the performance curve in Figure 2(a). In other words, the h where SGC-1 and GCN perform worst is where $g(h)$ gets the smallest value, instead of the point with the smallest edge homophily value $h = 0$. This again reveals the advantage of $H_{\text{agg}}(\mathcal{G})$ over $H_{\text{edge}}(\mathcal{G})$ by taking use of the similarity matrix.

4 Adaptive Channel Mixing (ACM) Framework

Besides the new homophily metrics, in this section, we will also figure out how diversification operation (high-pass filter) is potentially capable to address some cases of harmful heterophily based on the similarity matrix proposed in equation (5). From the analysis, we argue that low-pass filter and high-pass filter should be combined together for feature extraction, which lead us to the filterbank method in subsection 4.2. We generalize filterbank method and propose ACM framework in subsection 4.3.

³A similar J-shaped curve is found in [40], though using different data generation processes. It does not mention the insufficiency of edge homophily.

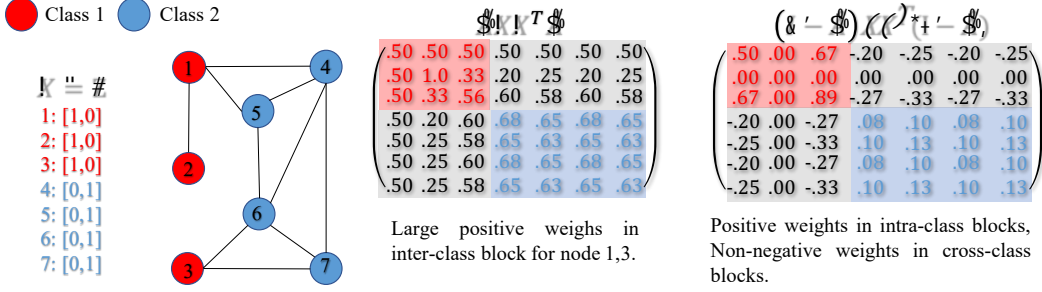


Figure 3: Example of how HP filter addresses harmful heterophily

4.1 How Diversification Operation Helps with Harmful Heterophily

We first consider the example shown in Figure 3. From $S(\hat{A}, X)$, nodes 1,3 assign relatively large positive weights to nodes in class 2 after aggregation, which will make node 1,3 hard to be distinguished from nodes in class 2. Despite the fact, we can still distinguish between nodes 1,3 and 4,5,6,7 by considering their neighborhood difference: nodes 1,3 are different from most of their neighbors while nodes 4,5,6,7 are similar to most of their neighbors. This indicates, in some cases, although some nodes become similar after aggregation, they are still distinguishable via their surrounding dissimilarities. This leads us to use *diversification operation*, i.e., high-pass (HP) filter $I - \hat{A}$ [10] (will be introduced in the next subsection) to extract the information of neighborhood differences and address harmful heterophily. As $S(I - \hat{A}, X)$ in Figure 3 shows, nodes 1,3 will assign negative weights to nodes 4,5,6,7 after diversification operation, i.e., nodes 1,3 treat nodes 4,5,6,7 as negative samples and will move away from them during backpropagation. Base on this example, we first propose diversification distinguishability as follows to measures the proportion of nodes that diversification operation is potentially helpful for,

Definition 2. *Diversification Distinguishability (DD) based on $S(I - \hat{A}, X)$.*

Given $S(I - \hat{A}, X)$, a node v is diversification distinguishable if the following two conditions are satisfied at the same time,

1. $\text{Mean}_u \left(\{S(I - \hat{A}, X)_{v,u} | u \in \mathcal{V} \wedge Z_{u,:} = Z_{v,:}\} \right) \geq 0;$
2. $\text{Mean}_u \left(\{S(I - \hat{A}, X)_{v,u} | u \in \mathcal{V} \wedge Z_{u,:} \neq Z_{v,:}\} \right) \leq 0$

(10)

Then, graph diversification distinguishability value is defined as

$$\text{DD}_{\hat{A},X}(\mathcal{G}) = \frac{1}{|\mathcal{V}|} \left| \{v | v \text{ is diversification distinguishable} \} \right| \quad (11)$$

We can see that $\text{DD}_{\hat{A},X}(\mathcal{G}) \in [0, 1]$. The effectiveness of diversification operation can be proved for binary classification problems under certain conditions based on definition 2, leading us to:

Theorem 2. (See Appendix E for proof). Suppose $X = Z, \hat{A} = \hat{A}_{\text{rw}}$. Then, for a binary classification problem, i.e., $C = 2$, all nodes are diversification distinguishable, i.e., $\text{DD}_{\hat{A},Z}(\mathcal{G}) = 1$.

Theorem 2 theoretically demonstrates the importance of diversification operation to extract high-frequency information of graph signal [10]. Combined with aggregation operation, which is a low-pass filter [10, 30], we can get a filterbank which uses both aggregation and diversification operations to distinctively extract the low- and high-frequency information from graph signals. We will introduce filterbank in the next subsection.

4.2 Filterbank in Spectral and Spatial Forms

Filterbank For the graph signal \mathbf{x} defined on \mathcal{G} , a 2-channel linear (analysis) filterbank [10]⁴ includes a pair of low-pass(LP) and high-pass(HP) filters H_{LP}, H_{HP} , where H_{LP} and H_{HP} retain the low-frequency and high-frequency content of \mathbf{x} , respectively.

Most existing GNNs are under uni-channel filtering architecture [18, 35, 15] with either H_{LP} or H_{HP} channel that only partially preserves the input information. Unlike the uni-channel architecture, filterbanks with $H_{LP} + H_{HP} = I$ will not lose any information of the input signal, *i.e.*, perfect reconstruction property [10].

Generally, the Laplacian matrices ($L_{\text{sym}}, L_{\text{rw}}, \hat{L}_{\text{sym}}, \hat{L}_{\text{rw}}$) can be regarded as HP filters [10] and affinity matrices ($A_{\text{sym}}, A_{\text{rw}}, \hat{A}_{\text{sym}}, \hat{A}_{\text{rw}}$) can be treated as LP filters [30, 14]. Moreover, MLPs can be considered as owing a special identity filterbank with matrix I that satisfies $H_{LP} + H_{HP} = I + 0 = I$.

Filterbank in Spatial Form Filterbank methods can also be extended to spatial GNNs. Formally, on the node level, left multiplying H_{LP} and H_{HP} on \mathbf{x} performs as aggregation and diversification operations, respectively. For example, suppose $H_{LP} = \hat{A}$ and $H_{HP} = I - \hat{A}$, then for node i we have

$$(H_{LP}\mathbf{x})_i = \sum_{j \in \{\mathcal{N}_i \cup i\}} \hat{A}_{i,j} \mathbf{x}_j, (H_{HP}\mathbf{x})_i = \mathbf{x}_i - \sum_{j \in \{\mathcal{N}_i \cup i\}} \hat{A}_{i,j} \mathbf{x}_j \quad (12)$$

where $\hat{A}_{i,j}$ is the connection weight between two nodes. To leverage HP and identity channels in GNNs, we propose the Adaptive Channel Mixing (ACM) architecture in the following subsection.

4.3 Adaptive Channel Mixing(ACM) GNN Framework

ACM framework can be applied to lots of baseline GNNs and in this subsection, we use GCN as an example and introduce ACM framework in matrix form. We use H_{LP} and H_{HP} to represent general LP and HP filters. The ACM framework includes 3 steps as follows,

Step 1. Feature Extraction for Each Channel:

Option 1: $H_L^l = \text{ReLU}(H_{LP}H^{l-1}W_L^{l-1})$, $H_H^l = \text{ReLU}(H_{HP}H^{l-1}W_H^{l-1})$, $H_I^l = \text{ReLU}(IH^{l-1}W_I^{l-1})$;
 Option 2: $H_L^l = H_{LP}\text{ReLU}(H^{l-1}W_L^{l-1})$, $H_H^l = H_{HP}\text{ReLU}(H^{l-1}W_H^{l-1})$, $H_I^l = I\text{ReLU}(H^{l-1}W_I^{l-1})$;
 $W_L^{l-1}, W_H^{l-1}, W_I^{l-1} \in \mathbb{R}^{F_{l-1} \times F_l}$;

Step 2. Feature-based Weight Learning

$\tilde{\alpha}_L^l = \sigma(H_L^l \tilde{W}_L^l)$, $\tilde{\alpha}_H^l = \sigma(H_H^l \tilde{W}_H^l)$, $\tilde{\alpha}_I^l = \sigma(H_I^l \tilde{W}_I^l)$, $\tilde{W}_L^{l-1}, \tilde{W}_H^{l-1}, \tilde{W}_I^{l-1} \in \mathbb{R}^{F_l \times 1}$
 $[\alpha_L^l, \alpha_H^l, \alpha_I^l] = \text{Softmax}([\tilde{\alpha}_L^l, \tilde{\alpha}_H^l, \tilde{\alpha}_I^l] W_{\text{Mix}}^l / T)$, $W_{\text{Mix}}^l \in \mathbb{R}^{3 \times 3}$, $T \in \mathbb{R}$ is the temperature;

Step 3. Node-wise Channel Mixing:

$$H^l = (\text{diag}(\alpha_L^l)H_L^l + \text{diag}(\alpha_H^l)H_H^l + \text{diag}(\alpha_I^l)H_I^l). \quad (13)$$

The framework with option 1 in step 1 is ACM framework and with option 2 is ACMII framework. ACM(II)-GCN first implement distinct feature extractions for 3 channels, respectively. After processed by a set of filterbanks, 3 filtered components H_L^l, H_H^l, H_I^l are obtained. Different nodes may have different needs for the information in the 3 channels, *e.g.*, in Figure 3, nodes 1,3 demand high-frequency information while node 2 only needs low-frequency information. To adaptively exploit information from different channels, ACM(II)-GCN learns row-wise (node-wise) feature-conditioned weights to combine the 3 channels. ACM(II) can be easily plugged into spatial GNNs by replacing H_{LP} and H_{HP} by aggregation and diversification operations as shown in (12). See Appendix F for a detailed discussion of model comparison on synthetic datasets.

Complexity Number of learnable parameters in layer l of ACM(II)-GCN is $3F_{l-1}(F_l + 1) + 9$, while it is $F_{l-1}F_l$ in GCN. The computation of step 1-3 takes $NF_l(8 + 6F_{l-1}) + 2F_l(\text{nnz}(H_{LP}) + \text{nnz}(H_{HP})) + 18N$ flops, while GCN layer takes $2NF_{l-1}F_l + 2F_l(\text{nnz}(H_{LP}))$ flops, where $\text{nnz}(\cdot)$ is the number of non-zero elements. A detailed comparison on running time is conducted in section 6.1.

⁴In graph signal processing, an additional synthesis filter [10] is required to form the 2-channel filterbank. But synthesis filter is not needed in our framework, so we do not introduce it in our paper.

Limitations Diversification operation does not work well in all harmful heterophily cases. For example, consider an imbalanced dataset where several small clusters with distinctive labels are densely connected to a large cluster. In this case, the surrounding differences of nodes in small clusters are similar, *i.e.*, the neighborhood differences are mainly from their connection to the same large cluster, and this possibly makes diversification operation fail to discriminate them. See a more detailed demonstration and discussion in Appendix G.

5 Prior Work

GNNs on Addressing Heterophily We discuss relevant work of GNNs on addressing heterophily challenge in this part. [1] acknowledges the difficulty of learning on graphs with weak homophily and propose MixHop to extract features from multi-hop neighborhood to get more information. Geom-GCN [33] precomputes unsupervised node embeddings and uses graph structure defined by geometric relationships in the embedding space to define the bi-level aggregation process. [16] proposes measurements based on feature smoothness and label smoothness that are potentially helpful to guide GNNs on dealing with heterophilous graphs. H₂GCN [40] combines 3 key designs to address heterophily: (1) ego- and neighbor-embedding separation; (2) higher-order neighborhoods; (3) combination of intermediate representations. CPGNN [39] models label correlations by the compatibility matrix, which is beneficial for heterophily settings, and propagates a prior belief estimation into GNNs by the compatibility matrix. FBGNN [29] first proposes to use filterbank to address heterophily problem, but it does not fully explain the insights behind HP filters and does not contain identity channel and node-wise channel mixing mechanism. FAGCN [4] learns edge-level aggregation weights as GAT [35] but allows the weights to be negative which enables the network to capture the high-frequency components in graph signals. GPRGNN [7] uses learnable weights that can be both positive and negative for feature propagation, it allows GRPGNN to adapt heterophily structure of graph and is able to handle both high- and low-frequency parts of the graph signals.

GNNs with Filterbanks Previously, there are geometric scattering networks [12, 32] that apply filterbanks to address over-smoothing [23] problem. The scattering construction captures different channels of variation from node features or labels. In geometric learning and graph signal processing, the band-pass filtering operations extract geometric information beyond smooth signals, thus it is believed that filterbanks can alleviate over-smoothing in GNNs. In ACM framework, we aim to design a framework with the help of filterbanks to adaptively utilize different channels to address the challenge of learning on heterophilous graph. We deal with different problem from [12, 32].

6 Experiments on Real-World Datasets

In this section, we evaluate ACM(II) framework on real-world datasets. We first conduct ablation studies in subsection 6.1 to validate different components. Then, we compare with the state-of-the-arts (SOTA) models in subsection 6.2.

6.1 Ablation Study & Efficiency

We investigate the effectiveness and efficiency of adding HP, identity channels and the adaptive mixing mechanism in ACM(II) framework by ablation study. Specifically, we apply the above components to SGC-1 and GCN separately, run 10 times on each dataset with 60%/20%/20% random splits for train/validation/test used in [7] and report the average test accuracy as well as the standard deviation. We also record the average running time per epoch (in milliseconds) to compare the efficiency. We set the temperature T in (13) to be 3. (See Appendix A for hyperparameter searching range.)

From the results we can see that on most datasets, the additional HP and identity channels are helpful, even on strong homophily datasets, such as Cora, CiteSeer and PubMed. The adaptive mixing mechanism also shows its advantage over the method that directly adds the three channels together. This illustrates the necessity of learning to customize the channel usage adaptively for different nodes. As for efficiency, we can see that the running time is approximately doubled under ACM(II) framework than the original model.

Ablation Study on Different Components in ACM-SGC and ACM-GCN (%)											
Baseline	Model Components	Cornell	Wisconsin	Texas	Film	Chameleon	Squirrel	Cora	CiteSeer	PubMed	Rank
Models	LP HP Identity Mixing	Acc \pm Std	Acc \pm Std	Acc \pm Std	Acc \pm Std	Acc \pm Std	Acc \pm Std	Acc \pm Std	Acc \pm Std	Acc \pm Std	Rank
SGC-1 w/	✓	70.98 \pm 8.39	70.38 \pm 2.85	83.28 \pm 5.43	25.26 \pm 1.18	64.86 \pm 1.81	47.62 \pm 1.27	85.12 \pm 1.64	79.66 \pm 0.75	85.5 \pm 0.76	12.89
	✓ ✓	83.28 \pm 5.81	91.88 \pm 1.61	90.98 \pm 2.46	36.76 \pm 1.01	65.27 \pm 1.9	47.27 \pm 1.37	86.8 \pm 1.08	80.98 \pm 1.68	87.21 \pm 0.42	10.44
	✓ ✓ ✓	93.93 \pm 3.6	95.25 \pm 1.84	93.93 \pm 2.54	38.38 \pm 1.13	63.83 \pm 2.07	46.79 \pm 0.75	86.73 \pm 1.28	80.57 \pm 0.99	87.8 \pm 0.58	9.44
	✓ ✓ ✓ ✓	88.2 \pm 4.39	93.5 \pm 2.95	92.95 \pm 2.94	37.19 \pm 0.87	62.82 \pm 1.84	44.94 \pm 0.93	85.22 \pm 1.35	80.75 \pm 1.68	88.11 \pm 0.21	11.00
ACM-GCN w/	✓	82.46 \pm 3.11	75.5 \pm 2.92	83.11 \pm 3.2	35.51 \pm 0.99	64.18 \pm 2.62	44.76 \pm 1.39	87.78 \pm 0.96	81.39 \pm 1.23	88.9 \pm 0.32	11.44
	✓ ✓	82.13 \pm 2.59	86.62 \pm 4.61	89.19 \pm 3.04	38.06 \pm 1.35	69.21 \pm 1.68	57.2 \pm 1.01	88.93 \pm 1.55	81.96 \pm 0.91	90.01 \pm 0.8	7.22
	✓ ✓ ✓	94.26 \pm 2.23	96.13 \pm 2.2	94.1 \pm 2.95	41.51 \pm 0.99	67.44 \pm 2.14	53.97 \pm 1.39	88.95 \pm 0.9	81.72 \pm 1.22	90.88 \pm 0.55	4.44
	✓ ✓ ✓ ✓	91.64 \pm 2	95.37 \pm 3.31	95.25 \pm 2.37	40.47 \pm 1.49	68.93 \pm 2.04	54.78 \pm 1.27	89.13 \pm 1.77	81.96 \pm 2.03	91.01 \pm 0.7	3.11
ACMII-GCN w/	✓ ✓	82.46 \pm 3.03	91.00 \pm 1.75	90.33 \pm 2.69	38.39 \pm 0.75	67.59 \pm 2.14	53.67 \pm 1.71	89.13 \pm 1.14	81.75 \pm 0.85	89.87 \pm 0.39	7.44
	✓ ✓ ✓	94.26 \pm 2.57	96.00 \pm 2.15	94.26 \pm 2.96	40.96 \pm 1.2	66.35 \pm 1.76	50.78 \pm 2.07	89.06 \pm 1.07	81.86 \pm 1.22	90.71 \pm 0.67	4.67
	✓ ✓ ✓ ✓	91.48 \pm 1.43	96.25 \pm 2.09	93.77 \pm 2.91	40.27 \pm 1.07	66.52 \pm 2.65	52.9 \pm 1.64	88.83 \pm 1.16	81.54 \pm 0.95	90.6 \pm 0.47	6.67
	✓ ✓ ✓ ✓ ✓	95.9 \pm 1.83	96.62 \pm 2.44	95.25 \pm 3.15	41.84 \pm 1.15	68.38 \pm 1.36	54.53 \pm 2.09	89.00 \pm 0.72	81.79 \pm 0.95	90.74 \pm 0.5	2.78
Comparison of Average Running Time Per Epoch(ms)											
SGC-1 w/	✓	2.53	2.83	2.5	3.18	3.48	4.65	3.47	3.43	4.04	
	✓ ✓	4.01	4.57	4.24	4.55	4.76	5.09	5.39	4.69	4.75	
	✓ ✓ ✓	3.88	4.01	4.04	4.43	4.06	4.5	4.38	3.82	4.16	
	✓ ✓ ✓ ✓	3.31	3.49	3.18	3.7	3.53	4.83	3.92	3.87	4.24	
ACM-GCN w/	✓	3.67	3.74	3.59	4.86	4.96	6.41	4.24	4.18	5.08	
	✓ ✓	6.63	8.06	7.89	8.11	7.8	9.39	7.82	7.38	8.74	
	✓ ✓ ✓	5.73	5.91	5.93	6.86	6.35	7.15	7.34	6.65	6.8	
	✓ ✓ ✓ ✓	5.16	5.25	5.2	5.93	5.64	8.02	5.73	5.65	6.16	
ACMII-GCN w/	✓ ✓	6.62	7.35	7.39	7.62	7.33	9.69	7.49	7.58	7.97	
	✓ ✓ ✓	6.3	6.05	6.26	6.87	6.44	6.5	6.14	7.21	6.6	
	✓ ✓ ✓ ✓	5.24	5.27	5.46	5.72	5.65	7.87	5.48	5.65	6.33	
	✓ ✓ ✓ ✓ ✓	7.59	8.28	8.06	8.85	8	10	8.27	8.5	8.68	

Table 1: Ablation study on 9 real-world datasets [33]. Cell with ✓ means the component is applied to the baseline model. The best test results are highlighted.

6.2 Comparison with State-of-the-art Models

Datasets & Experimental Setup In this section, we implement SGC [36] with 1 hop and 2 hops (SGC-1, SGC-2), GCNII [6], GCNII* [6], GCN [18] and snowball networks with 2 and 3 layers (snowball-2, snowball-3) and apply them in ACM or ACMII framework (see details in appendix A.5): we use \hat{A}_{rw} as LP filter and the corresponding HP filter can be derived from (12). We compare them with several baselines and SOTA models: MLP with 2 layers (MLP-2), GAT [35], APPNP [19], GPRGNN [7], H₂GCN [40], MixHop [1], GCN+JK [18, 37, 24], GAT+JK [35, 37, 24], FAGCN [4] GraphSAGE [15] and Geom-GCN [33]. Besides the 9 benchmark datasets used in [33], we further test the above models on a new benchmark dataset, *Deezer-Europe*, that is proposed in [24]. We test these models 10 times on *Cornell*, *Wisconsin*, *Texas*, *Film*, *Chameleon*, *Squirrel*, *Cora*, *Citeseer* and *Pubmed* following the same early stopping strategy, the same random data splitting method⁵ and Adam [17] optimizer as used in GPRGNN [7]. For *Deezer-Europe*, we test the above models 5 times with the same early stopping strategy, the same fixed splits and AdamW [27] used in [24]. The details of hyperparameter searching range and the optimal hyperparameters are reported in appendix A.3 and A.4.

The main results of this set of experiments with statistics of datasets are summarized in Table 2, where we report the mean accuracy and standard deviation. We can see that after applied in ACM(II) framework, the performance of baseline models are boosted on almost all tasks. Especially, ACMII-GCN performs the best in terms of average rank (3.40) across all datasets and ACM(II)-GNNs achieve SOTA performance on 8 out of 10 datasets. Overall, It suggests that ACM(II) framework can help GNNs to generalize better on node classification tasks on heterophilous graphs.

⁵See the open source code for splits in <https://github.com/jianhao2016/GPRGNN/blob/f4aaad6ca28c83d3121338a4c4fe5d162edfa9a2/src/utis.py#L16>. See table 9 in appendix I for the performance comparison with several SOTA models on the fixed 48%/32%/20% splits provided by [33].

	Cornell	Wisconsin	Texas	Film	Chameleon	Squirrel	Deezer-Europe	Cora	CiteSeer	PubMed	
#nodes	183	251	183	7,600	2,277	5,201	28,281	2,708	3,327	19,717	
#edges	295	499	309	33,544	36,101	217,073	92,752	5,429	4,732	44,338	
#features	1,703	1,703	1,703	931	2,325	2,089	31,241	1,433	3,703	500	
#classes	5	5	5	5	5	5	2	7	6	3	
H _{edge}	0.5669	0.4480	0.4106	0.3750	0.2795	0.2416	0.5251	0.8100	0.7362	0.8024	
H _{node}	0.3855	0.1498	0.0968	0.2210	0.2470	0.2156	0.5299	0.8252	0.7175	0.7924	
H _{class}	0.0468	0.0941	0.0013	0.0110	0.0620	0.0254	0.0304	0.7657	0.6270	0.6641	
Data Splits	60%/20%/20%	60%/20%/20%	60%/20%/20%	60%/20%/20%	60%/20%/20%	60%/20%/20%	50%/25%/25%	60%/20%/20%	60%/20%/20%	60%/20%/20%	
H _{agg} M(G)	0.8032	0.7768	0.694	0.6822	0.61	0.3566	0.5790	0.9904	0.9826	0.9432	
Test Accuracy (%) of State-of-the-art Models, Baseline GNN Models and ACM-GNN models											Rank
MLP-2*	91.30 ± 0.70	93.87 ± 3.33	92.26 ± 0.71	38.58 ± 0.25	46.72 ± 0.46	31.28 ± 0.27	66.55 ± 0.72	76.44 ± 0.30	76.25 ± 0.28	86.43 ± 0.13	18.60
GAT*	76.00 ± 1.01	71.01 ± 4.66	78.87 ± 0.86	35.98 ± 0.23	63.9 ± 0.46	42.72 ± 0.33	61.09 ± 0.77	76.70 ± 0.42	67.20 ± 0.46	83.28 ± 0.12	21.40
APPNP*	91.80 ± 0.63	92.00 ± 3.59	91.18 ± 0.70	38.86 ± 0.24	51.91 ± 0.56	34.77 ± 0.34	67.21 ± 0.56	79.41 ± 0.38	68.59 ± 0.30	85.02 ± 0.09	18.00
GPRGNN*	91.36 ± 0.70	93.75 ± 2.37	92.92 ± 0.61	39.30 ± 0.27	67.48 ± 0.40	49.93 ± 0.53	66.90 ± 0.50	79.51pm 0.36	67.63 ± 0.38	85.07 ± 0.09	14.40
H2GCN	86.23 ± 4.71	87.5 ± 1.77	85.90 ± 3.53	38.85 ± 1.17	52.30 ± 0.48	30.39 ± 1.22	67.22 ± 0.90	87.52 ± 0.61	79.97 ± 0.69	87.78 ± 0.28	17.00
MixHop	60.33 ± 28.53	77.25 ± 7.80	76.39 ± 7.66	33.13 ± 2.40	36.28 ± 10.22	24.55 ± 2.60	66.80 ± 0.58	65.65 ± 11.31	49.52 ± 13.35	87.04 ± 4.10	23.50
GCN+JK	66.56 ± 13.82	62.50 ± 15.75	80.66 ± 1.91	32.72 ± 2.62	64.68 ± 2.85	53.40 ± 1.90	60.99 ± 0.14	86.90 ± 1.51	73.77 ± 1.85	90.09 ± 0.68	18.80
GAT+JK	74.43 ± 10.24	69.50 ± 3.12	75.41 ± 7.18	35.41 ± 0.97	68.14 ± 1.18	52.28 ± 3.61	59.66 ± 0.92	89.52 ± 0.43	74.49 ± 2.76	89.15 ± 0.87	16.70
FAGCN	88.03 ± 5.6	89.75 ± 6.37	88.85 ± 4.39	31.59 ± 1.37	49.47 ± 2.84	42.24 ± 1.2	66.86 p. 0.53	88.85 ± 1.36	82.37 ± 1.46	89.98 ± 0.54	14.10
GraphSAGE	71.41 ± 1.24	64.85 ± 5.14	79.03 ± 1.20	36.37 ± 0.21	62.15 ± 0.42	41.26 ± 0.26	OOM	86.58 ± 0.26	78.24 ± 0.30	86.85 ± 0.11	20.89
Geom-GCN†	60.81	64.12	67.57	31.63	60.9	38.14	NA	85.27	77.99	90.05	22.67
SGC-1	70.98 ± 8.39	70.38 ± 2.85	83.28 ± 5.43	25.26 ± 1.18	64.86 ± 1.81	47.62 ± 1.27	59.73 ± 0.12	85.12 ± 1.64	79.66 ± 0.75	85.5 ± 0.76	20.10
SGC-2	72.62 ± 9.92	74.75 ± 2.89	81.31 ± 3.3	28.81 ± 1.11	62.67 ± 2.41	41.25 ± 1.4	61.56 ± 0.51	85.48 ± 1.48	80.75 ± 1.15	85.36 ± 0.52	20.70
GCNII	89.18 ± 3.96	83.25 ± 2.69	82.46 ± 4.58	40.82 ± 1.79	60.35 ± 2.7	38.81 ± 1.97	66.38 ± 0.45	88.98 ± 1.33	81.58 ± 1.3	89.8 ± 0.3	14.80
GCNII*	90.49 ± 4.45	89.12 ± 3.06	88.52 ± 3.02	41.54 ± 0.99	62.8 ± 2.87	38.31 ± 1.3	66.42 ± 0.56	88.93 ± 1.37	81.83 ± 1.78	89.98 ± 0.52	12.30
GCN	82.46 ± 3.11	75.5 ± 2.92	83.11 ± 3.2	35.51 ± 0.99	64.18 ± 2.62	44.76 ± 1.39	62.23 ± 0.53	87.78 ± 0.96	81.39 ± 1.23	88.9 ± 0.32	16.30
Snowball-2	82.62 ± 2.34	74.88 ± 3.42	83.11 ± 3.2	35.97 ± 0.66	64.99 ± 2.39	47.88 ± 1.23	OOM	88.64 ± 1.15	81.53 ± 1.71	89.04 ± 0.49	15.22
Snowball-3	82.95 ± 2.1	69.5 ± 5.01	83.11 ± 3.2	36.00 ± 1.36	65.49 ± 1.64	48.25 ± 0.94	OOM	89.33 ± 1.3	80.93 ± 1.32	88.8 ± 0.82	14.78
ACM-SGC-1	93.77 ± 1.91	93.25 ± 2.92	93.61 ± 1.55	39.33 ± 1.25	63.68 ± 1.62	46.4 ± 1.13	66.67 ± 0.56	86.63 ± 1.13	80.96 ± 0.93	87.75 ± 0.88	12.60
ACM-SGC-2	93.77 ± 2.17	94.00 ± 2.61	93.44 ± 2.54	40.13 ± 1.21	60.48 ± 1.55	40.91 ± 1.39	66.53 ± 0.57	87.64 ± 0.99	80.93 ± 1.16	88.79 ± 0.5	13.40
ACM-GCNII	92.62 ± 3.13	94.63 ± 2.96	92.46 ± 1.97	41.37 ± 1.37	58.73 ± 2.52	40.9 ± 1.58	66.39 ± 0.56	89.1 ± 1.61	82.28 ± 1.12	90.12 ± 0.4	10.40
ACM-GCNII*	93.44 ± 2.74	94.37 ± 2.81	93.28 ± 2.79	41.27 ± 1.24	61.66 ± 2.29	38.32 ± 1.5	66.6 ± 0.57	89.00 ± 1.35	81.69 ± 1.25	90.18 ± 0.51	10.10
ACM-GCN	94.75 ± 3.8	95.75 ± 2.03	94.92 ± 2.88	41.62 ± 1.15	69.04 ± 1.74	58.02 ± 1.86	67.01 ± 0.38	88.62 ± 1.22	81.68 ± 0.97	90.66 ± 0.47	4.80
ACM-Snowball-2	95.08 ± 3.11	96.38 ± 2.59	95.74 ± 2.22	41.4 ± 1.23	68.51 ± 1.7	55.97 ± 2.03	OOM	88.83 ± 1.49	81.58 ± 1.23	90.81 ± 0.52	4.44
ACM-Snowball-3	94.26 ± 2.57	96.62 ± 1.86	94.75 ± 2.41	41.27 ± 0.8	68.4 ± 2.05	55.73 ± 2.39	OOM	89.59 ± 1.58	81.32 ± 0.97	91.44 ± 0.59	4.44
ACMII-GCN	95.9 ± 1.83	96.62 ± 2.44	95.08 ± 2.07	41.84 ± 1.15	68.38 ± 1.36	54.53 ± 2.09	67.15 ± 0.41	89.00 ± 0.72	81.79 ± 0.95	90.74 ± 0.5	3.40
ACMII-Snowball-2	95.25 ± 1.55	96.63 ± 2.24	95.25 ± 1.55	41.1 ± 0.75	67.83 ± 2.63	53.48 ± 0.6	OOM	88.95 ± 1.04	82.07 ± 1.04	90.56 ± 0.39	4.78
ACMII-Snowball-3	93.61 ± 2.79	97.00 ± 2.63	94.75 ± 3.09	40.31 ± 1.6	67.53 ± 2.83	52.31 ± 1.57	OOM	89.36 ± 1.26	81.56 ± 1.15	91.31 ± 0.6	5.89

Table 2: Experimental results: average test accuracy \pm standard deviation on 10 real-world benchmark datasets. The best results are highlighted. Results "*" are reported from [7, 24] and results "†" are from [33]. NA means the reported results are not available and OOM means out of memory.

7 Future Work

The similarity matrix and the new metrics defined in this paper mainly capture the linear relations of the aggregated node features. But this might be insufficient sometimes when nonlinearity information in feature vectors are important for classification. In the future, similarity matrix that is able to capture nonlinear relations between node features can be proposed to define new homophily metrics.

As the limitation raised in section 4.3, filterbank method cannot properly handle all cases of harmful heterophily. In the future, we need to explore and address more challenging heterophilous graph with GNNs.

References

- [1] S. Abu-El-Haija, B. Perozzi, A. Kapoor, N. Alipourfard, K. Lerman, H. Harutyunyan, G. Ver Steeg, and A. Galstyan. Mixhop: Higher-order graph convolutional architectures via sparsified neighborhood mixing. In *international conference on machine learning*, pages 21–29. PMLR, 2019.
- [2] D. Bahdanau, K. Cho, and Y. Bengio. Neural machine translation by jointly learning to align and translate. *arXiv preprint arXiv:1409.0473*, 2014.
- [3] P. W. Battaglia, J. B. Hamrick, V. Bapst, A. Sanchez-Gonzalez, V. Zambaldi, M. Malinowski, A. Tacchetti, D. Raposo, A. Santoro, R. Faulkner, et al. Relational inductive biases, deep learning, and graph networks. *arXiv preprint arXiv:1806.01261*, 2018.
- [4] D. Bo, X. Wang, C. Shi, and H. Shen. Beyond low-frequency information in graph convolutional networks. *arXiv preprint arXiv:2101.00797*, 2021.
- [5] M. M. Bronstein, J. Bruna, Y. LeCun, A. Szlam, and P. Vandergheynst. Geometric deep learning: going beyond euclidean data. *arXiv*, abs/1611.08097, 2016.
- [6] M. Chen, Z. Wei, Z. Huang, B. Ding, and Y. Li. Simple and deep graph convolutional networks. In *International Conference on Machine Learning*, pages 1725–1735. PMLR, 2020.
- [7] E. Chien, J. Peng, P. Li, and O. Milenkovic. Adaptive universal generalized pagerank graph neural network. In *International Conference on Learning Representations*. <https://openreview.net/forum>, 2021.
- [8] F. R. Chung and F. C. Graham. *Spectral graph theory*. Number 92. American Mathematical Soc., 1997.
- [9] M. Defferrard, X. Bresson, and P. Vandergheynst. Convolutional neural networks on graphs with fast localized spectral filtering. *arXiv*, abs/1606.09375, 2016.
- [10] V. N. Ekambaram. *Graph structured data viewed through a fourier lens*. University of California, Berkeley, 2014.
- [11] M. Fey and J. E. Lenssen. Fast graph representation learning with pytorch geometric. *arXiv preprint arXiv:1903.02428*, 2019.
- [12] F. Gao, G. Wolf, and M. Hirn. Geometric scattering for graph data analysis. In *International Conference on Machine Learning*, pages 2122–2131. PMLR, 2019.
- [13] A. Graves, A.-r. Mohamed, and G. Hinton. Speech recognition with deep recurrent neural networks. In *2013 IEEE international conference on acoustics, speech and signal processing*, pages 6645–6649. Ieee, 2013.
- [14] W. L. Hamilton. Graph representation learning. *Synthesis Lectures on Artificial Intelligence and Machine Learning*, 14(3):1–159, 2020.
- [15] W. L. Hamilton, R. Ying, and J. Leskovec. Inductive representation learning on large graphs. *arXiv*, abs/1706.02216, 2017.
- [16] Y. Hou, J. Zhang, J. Cheng, K. Ma, R. T. Ma, H. Chen, and M.-C. Yang. Measuring and improving the use of graph information in graph neural networks. In *International Conference on Learning Representations*, 2019.
- [17] D. P. Kingma and J. Ba. Adam: A method for stochastic optimization. *arXiv preprint arXiv:1412.6980*, 2014.
- [18] T. N. Kipf and M. Welling. Semi-supervised classification with graph convolutional networks. *arXiv*, abs/1609.02907, 2016.
- [19] J. Klicpera, A. Bojchevski, and S. Günnemann. Predict then propagate: Graph neural networks meet personalized pagerank. *arXiv preprint arXiv:1810.05997*, 2018.
- [20] A. Krizhevsky, I. Sutskever, and G. E. Hinton. Imagenet classification with deep convolutional neural networks. In *Advances in neural information processing systems*, pages 1097–1105, 2012.
- [21] Y. LeCun, Y. Bengio, and G. Hinton. Deep learning. *nature*, 521(7553):436, 2015.
- [22] Y. LeCun, L. Bottou, Y. Bengio, P. Haffner, et al. Gradient-based learning applied to document recognition. *Proceedings of the IEEE*, 86(11):2278–2324, 1998.

- [23] Q. Li, Z. Han, and X. Wu. Deeper insights into graph convolutional networks for semi-supervised learning. *arXiv*, abs/1801.07606, 2018.
- [24] D. Lim, X. Li, F. Hohne, and S.-N. Lim. New benchmarks for learning on non-homophilous graphs. *arXiv preprint arXiv:2104.01404*, 2021.
- [25] V. Lingam, R. Ragesh, A. Iyer, and S. Sellamanickam. Simple truncated svd based model for node classification on heterophilic graphs. *arXiv preprint arXiv:2106.12807*, 2021.
- [26] M. Liu, Z. Wang, and S. Ji. Non-local graph neural networks. *arXiv preprint arXiv:2005.14612*, 2020.
- [27] I. Loshchilov and F. Hutter. Decoupled weight decay regularization. *arXiv preprint arXiv:1711.05101*, 2017.
- [28] S. Luan, M. Zhao, X.-W. Chang, and D. Precup. Break the ceiling: Stronger multi-scale deep graph convolutional networks. *arXiv preprint arXiv:1906.02174*, 2019.
- [29] S. Luan, M. Zhao, C. Hua, X.-W. Chang, and D. Precup. Complete the missing half: Augmenting aggregation filtering with diversification for graph convolutional networks. *arXiv preprint arXiv:2008.08844*, 2020.
- [30] T. Maehara. Revisiting graph neural networks: All we have is low-pass filters. *arXiv preprint arXiv:1905.09550*, 2019.
- [31] M. McPherson, L. Smith-Lovin, and J. M. Cook. Birds of a feather: Homophily in social networks. *Annual review of sociology*, 27(1):415–444, 2001.
- [32] Y. Min, F. Wenkel, and G. Wolf. Scattering gcn: Overcoming oversmoothness in graph convolutional networks. *arXiv preprint arXiv:2003.08414*, 2020.
- [33] H. Pei, B. Wei, K. C.-C. Chang, Y. Lei, and B. Yang. Geom-gcn: Geometric graph convolutional networks. *arXiv preprint arXiv:2002.05287*, 2020.
- [34] F. Scarselli, M. Gori, A. C. Tsoi, M. Hagenbuchner, and G. Monfardini. The graph neural network model. *IEEE transactions on neural networks*, 20(1):61–80, 2008.
- [35] P. Velickovic, G. Cucurull, A. Casanova, A. Romero, P. Lio, and Y. Bengio. Graph attention networks. *arXiv*, abs/1710.10903, 2017.
- [36] F. Wu, T. Zhang, A. H. d. Souza Jr, C. Fifty, T. Yu, and K. Q. Weinberger. Simplifying graph convolutional networks. *arXiv preprint arXiv:1902.07153*, 2019.
- [37] K. Xu, C. Li, Y. Tian, T. Sonobe, K.-i. Kawarabayashi, and S. Jegelka. Representation learning on graphs with jumping knowledge networks. In J. Dy and A. Krause, editors, *Proceedings of the 35th International Conference on Machine Learning*, volume 80 of *Proceedings of Machine Learning Research*, pages 5453–5462. PMLR, 10–15 Jul 2018.
- [38] Y. Yan, M. Hashemi, K. Swersky, Y. Yang, and D. Koutra. Two sides of the same coin: Heterophily and oversmoothing in graph convolutional neural networks. *arXiv preprint arXiv:2102.06462*, 2021.
- [39] J. Zhu, R. A. Rossi, A. Rao, T. Mai, N. Lipka, N. K. Ahmed, and D. Koutra. Graph neural networks with heterophily. *arXiv preprint arXiv:2009.13566*, 2020.
- [40] J. Zhu, Y. Yan, L. Zhao, M. Heimann, L. Akoglu, and D. Koutra. Beyond homophily in graph neural networks: Current limitations and effective designs. *Advances in Neural Information Processing Systems*, 33, 2020.

Checklist

1. For all authors...
 - (a) Do the main claims made in the abstract and introduction accurately reflect the paper's contributions and scope? [Yes]
 - (b) Did you describe the limitations of your work? [Yes] In the Appendix G, we discuss cases that high-pass filter cannot tackle.
 - (c) Did you discuss any potential negative societal impacts of your work? [No] It is in Section 8, we have not come up with significant social negative impact.
 - (d) Have you read the ethics review guidelines and ensured that your paper conforms to them? [Yes]
2. If you are including theoretical results...
 - (a) Did you state the full set of assumptions of all theoretical results? [Yes] In Section 3&4, we mainly define a new homophily metric and it is followed by two theorems.
 - (b) Did you include complete proofs of all theoretical results? [Yes] In Appendix B&D&E, we justify the new metric and two theorems.
3. If you ran experiments...
 - (a) Did you include the code, data, and instructions needed to reproduce the main experimental results (either in the supplemental material or as a URL)? [Yes] The settings are provided in details and the source code is submitted in the supplemental material.
 - (b) Did you specify all the training details (e.g., data splits, hyperparameters, how they were chosen)? [Yes] In Section 6, we specify model details.
 - (c) Did you report error bars (e.g., with respect to the random seed after running experiments multiple times)? [Yes] We include average test accuracy of times of running with standard deviation.
 - (d) Did you include the total amount of compute and the type of resources used (e.g., type of GPUs, internal cluster, or cloud provider)? [Yes] We include hardware details in Appendix, which is not computationally expensive.
4. If you are using existing assets (e.g., code, data, models) or curating/releasing new assets...
 - (a) If your work uses existing assets, did you cite the creators? [Yes] In Section 6, we specify the datasets with their data split sources in footnotes.
 - (b) Did you mention the license of the assets? [No]
 - (c) Did you include any new assets either in the supplemental material or as a URL? [No]
 - (d) Did you discuss whether and how consent was obtained from people whose data you're using/curating? [No]
 - (e) Did you discuss whether the data you are using/curating contains personally identifiable information or offensive content? [No] None included.
5. If you used crowdsourcing or conducted research with human subjects...
 - (a) Did you include the full text of instructions given to participants and screenshots, if applicable? [No] None included.
 - (b) Did you describe any potential participant risks, with links to Institutional Review Board (IRB) approvals, if applicable? [No] None included.
 - (c) Did you include the estimated hourly wage paid to participants and the total amount spent on participant compensation? [No] None included.

A Hyperparameters & Details of The Experiments

A.1 Hyperparameters Searching Range for GNNs on Synthetic Graphs

Hyperparameter Searching Range for Synthetic Experiments				
Models\Hyperparameters	lr	weight_decay	dropout	hidden
MLP-1	0.05	{5e-5, 1e-4, 5e-4}	-	-
SGC-1	0.05	{5e-5, 1e-4, 5e-4}	-	-
ACM-SGC-1	0.05	{5e-5, 1e-4, 5e-4}	{ 0.1, 0.2, 0.3, 0.4, 0.5, 0.6, 0.7,0.8,0.9}	-
MLP-2	0.05	{5e-5, 1e-4, 5e-4}	{ 0.1, 0.2, 0.3, 0.4, 0.5, 0.6, 0.7,0.8,0.9}	64
GCN	0.05	{5e-5, 1e-4, 5e-4}	{ 0.1, 0.2, 0.3, 0.4, 0.5, 0.6, 0.7,0.8,0.9}	64
ACM-GCN	0.05	{5e-5, 1e-4, 5e-4}	{ 0.1, 0.2, 0.3, 0.4, 0.5, 0.6, 0.7,0.8,0.9}	64

Table 3: Hyperparameter Searching Range for Synthetic Experiments

A.2 Hyperparameters Searching Range for GNNs on Ablation Study

Hyperparameter Searching Range for Ablation Study				
Models\Hyperparameters	lr	weight_decay	dropout	hidden
SGC-LP+HP	{0.01, 0.05, 0.1}	{0, 5e-6, 1e-5, 5e-5, 1e-4, 5e-4, 1e-3, 5e-3, 1e-2}	-	-
SGC-LP+Identity	{0.01, 0.05, 0.1}	{0, 5e-6, 1e-5, 5e-5, 1e-4, 5e-4, 1e-3, 5e-3, 1e-2}	-	-
ACM-SGC-no adaptive mixing	{0.01, 0.05, 0.1}	{0, 5e-6, 1e-5, 5e-5, 1e-4, 5e-4, 1e-3, 5e-3, 1e-2}	{0, 0.1, 0.2, 0.3, 0.4, 0.5, 0.6, 0.7,0.8,0.9}	-
GCN-LP+HP	{0.01, 0.05, 0.1}	{0, 5e-6, 1e-5, 5e-5, 1e-4, 5e-4, 1e-3, 5e-3, 1e-2}	{0, 0.1, 0.2, 0.3, 0.4, 0.5, 0.6, 0.7,0.8,0.9}	64
GCN-LP+Identity	{0.01, 0.05, 0.1}	{0, 5e-6, 1e-5, 5e-5, 1e-4, 5e-4, 1e-3, 5e-3, 1e-2}	{0, 0.1, 0.2, 0.3, 0.4, 0.5, 0.6, 0.7,0.8,0.9}	64
ACM-GCN-no adaptive mixing	{0.01, 0.05, 0.1}	{0, 5e-6, 1e-5, 5e-5, 1e-4, 5e-4, 1e-3, 5e-3, 1e-2}	{0, 0.1, 0.2, 0.3, 0.4, 0.5, 0.6, 0.7,0.8,0.9}	64

Table 4: Hyperparameter Searching Range for Ablation Study

A.3 Hyperparameters Searching Range for GNNs on Real-world Datasets

See table 5.

A.4 Optimal Hyperparameters for Baselines and ACM(II)-GNNs on Real-world Tasks

See table 6 and 7.

A.5 Details of the Implementation of ACM and ACMII Frameworks

In ACM(II) framework, we first use dropout operation over the input data. The implementation of ACM(II)-GCN and ACM(II)-snowball is straightforward, but SGC-1, SGC-2, GCNII and GCNII* are not able to be applied under ACM(II) framework and we will make an explanation as follows.

- SGC-1 and SGC-2: SGC does not contain nonlinearity, so the option 1 and option 2 in step 1 is the same for ACM-SGC and ACMII-SGC. Thus, we only implement ACM-SGC.
- GCNII and GCNII*:

$$\text{GCCII: } \mathbf{H}^{(\ell+1)} = \sigma \left(\left((1 - \alpha_\ell) \hat{\mathbf{A}} \mathbf{H}^{(\ell)} + \alpha_\ell \mathbf{H}^{(0)} \right) \left((1 - \beta_\ell) \mathbf{I}_n + \beta_\ell \mathbf{W}^{(\ell)} \right) \right)$$

$$\text{GCCII*}: \mathbf{H}^{(\ell+1)} = \sigma \left((1 - \alpha_\ell) \hat{\mathbf{A}} \mathbf{H}^{(\ell)} \left((1 - \beta_\ell) \mathbf{I}_n + \beta_\ell \mathbf{W}_1^{(\ell)} \right) + \alpha_\ell \mathbf{H}^{(0)} \left((1 - \beta_\ell) \mathbf{I}_n + \beta_\ell \mathbf{W}_2^{(\ell)} \right) \right)$$

Without major modification, GCNII and GCNII* are hard to be put into ACMII framework. In ACMII frameworks, before apply the operator \hat{A} , we first implement a nonlinear feature operation over H^ℓ . But in GCNII and GCNII*, before multiplying W^ℓ (or W_1^ℓ, W_2^ℓ) to extract features, we need to add another term including $H^{(0)}$, which are not filtered by \hat{A} . This is incompatible with ACMII framework, thus, we did not implement GCNII and GCNII* in ACMII framework.

The open source code will be released soon.

Models/Hyperparameters	lr	weight_decay	dropout	hidden	lambda	alpha_l	head	layers	JK type
H2GCN	0.01	0.001	{0, 0.5}	{8, 16, 32, 64}	-	-	-	{1, 2}	-
MixHop	0.01	0.001	0.5	{8, 16, 32}	-	-	-	{2, 3}	-
GCN+JK	{0.1, 0.01, 0.001}	0.001	0.5	{4, 8, 16, 32, 64}	-	-	-	2	{max, cat}
GAT+JK	{0.1, 0.01, 0.001}	0.001	0.5	{4, 8, 12, 32}	-	-	{2,4,8}	2	{max, cat}
GCNII, GCNII*	0.01	{0, 5e-6, 1e-5, 5e-5, 1e-4, 5e-4, 1e-3} for Deezer-Europe and {0, 5e-6, 1e-5, 5e-5, 1e-4, 5e-4, 1e-3, 5e-3, 1e-2} for others	0.5	64	{0.5, 1, 1.5}	{0.1,0.2,0.3,0.4,0.5}	-	{4, 8, 16, 32} for Deezer-Europe and {4, 8, 16, 32, 64} for others	-
Baselines: {SGC-1, SGC-2, GCN, Snowball-2, Snowball-3, FAGCN}; ACM-{SGC-1, SGC-2, GCN, Snowball-2, Snowball-3}; ACMII-{SGC-1, SGC-2, GCN, Snowball-2, Snowball-3}	{0.002, 0.01, 0.05} for Deezer-Europe and {0.01, 0.05, 0.1} for others	{0, 5e-6, 1e-5, 5e-5, 1e-4, 5e-4, 1e-3} for Deezer-Europe and {0, 5e-6, 1e-5, 5e-5, 1e-4, 5e-4, 1e-3, 5e-3, 1e-2} for others	{0, 0.1, 0.2, 0.3, 0.4, 0.5, 0.6, 0.7, 0.8, 0.9}	64	-	-	-	-	-
GraphSAGE	{0.01,0.05, 0.1}	{0, 5e-6, 1e-5, 5e-5, 1e-4, 5e-4, 1e-3} for Deezer-Europe and {0, 5e-6, 1e-5, 5e-5, 1e-4, 5e-4, 1e-3, 5e-3, 1e-2} for others	{0, 0.1, 0.2, 0.3, 0.4, 0.5, 0.6, 0.7, 0.8, 0.9}	8 for Deezer-Europe and 64 for others	-	-	-	-	-
ACM-{GCNII, GCNII*}	0.01	{0, 5e-6, 1e-5, 5e-5, 1e-4, 5e-4, 1e-3} for Deezer-Europe and {0, 5e-6, 1e-5, 5e-5, 1e-4, 5e-4, 1e-3, 5e-3, 1e-2} for others	{0, 0.1, 0.2, 0.3, 0.4, 0.5, 0.6, 0.7, 0.8, 0.9}	64	-	-	-	{1,2,3,4}	-

Table 5: Hyperparameter Searching Range for Real-world Datasets

A.6 Computing Resources

For all experiments on synthetic datasets and real-world datasets, we use NVidia V100 GPUs with 16/32GB GPU memory, 8-core CPU, 16G Memory. The software implementation is based on PyTorch and PyTorch Geometric [11].

Hyperparameters for Baseline GNNs														
Datasets	Models	Hyperparameters	lr	weight_decay	dropout	hidden	# layers	Gat heads	JK Type	lambda	alpha_1	results	std	average epoch time/average total time
Cornell	SGC-1	0.05	1.00E-02	0	64	-	-	-	-	-	-	70.98	8.39	2.53ms/0.51s
	SGC-2	0.05	1.00E-03	0	64	-	-	-	-	-	-	72.62	9.92	2.46ms/0.53s
	GCN	0.1	5.00E-03	0.5	64	2	-	-	-	-	-	82.46	3.11	3.67ms/0.74s
	Snowball-2	0.01	5.00E-03	0.4	64	2	-	-	-	-	-	82.62	2.34	4.24ms/0.87s
	Snowball-3	0.01	5.00E-03	0.4	64	3	-	-	-	-	-	82.95	2.1	6.66ms/1.36s
	GCNII	0.01	1.00E-03	0.5	64	16	-	-	-	0.5	0.5	89.18	3.96	25.41ms/8.11s
	GCNII*	0.01	1.00E-03	0.5	64	8	-	-	-	0.5	0.5	90.49	4.45	15.35ms/4.05s
	FAGCN	0.01	1.00E-04	0.7	32	2	-	-	-	-	-	88.03	5.6	8.1ms/3.8858s
	Mixhop	0.01	0.001	0.5	16	2	-	-	-	-	-	60.33	28.53	10.379ms/2.105s
	H2GCN	0.01	0.001	0.5	64	1	-	-	-	-	-	86.23	4.71	4.381ms/1.123s
	GCN+JK	0.1	0.001	0.5	64	2	-	-	cat	-	-	66.56	13.82	5.589ms/1.227s
	GAT+JK	0.1	0.001	0.5	32	2	8	max	-	-	-	74.43	10.24	10.725ms/2.478s
Wisconsin	SGC-1	0.05	5.00E-03	0	64	-	-	-	-	-	-	70.38	2.85	2.83ms/0.57s
	SGC-2	0.1	1.00E-03	0	64	-	-	-	-	-	-	74.75	2.89	2.14ms/0.43s
	GCN	0.1	1.00E-03	0.7	64	2	-	-	-	-	-	75.5	2.92	3.74ms/0.76s
	Snowball-2	0.1	1.00E-03	0.5	64	2	-	-	-	-	-	74.88	3.42	3.73ms/0.76s
	Snowball-3	0.05	5.00E-04	0.8	64	3	-	-	-	-	-	69.5	5.01	5.46ms/1.12s
	GCNII	0.01	1.00E-03	0.5	64	8	-	-	-	0.5	0.5	83.25	2.69	9.26ms/1.96s
	GCNII*	0.01	1.00E-03	0.5	64	4	-	-	-	1.5	0.3	89.12	3.06	12.9ms/4.6359s
	FAGCN	0.05	1.00E-04	0	32	2	-	-	-	-	-	89.75	6.37	10.281ms/2.095s
	Mixhop	0.01	0.001	0.5	16	2	-	-	-	-	-	77.25	7.80	4.324ms/1.134s
	H2GCN	0.01	0.001	0.5	32	1	-	-	-	-	-	87.5	1.77	5.117ms/1.049s
	GCN+JK	0.1	0.001	0.5	32	2	-	-	cat	-	-	62.5	15.75	10.762ms/2.25s
	GAT+JK	0.1	0.001	0.5	4	2	8	max	-	-	-	69.5	3.12	10.303ms/2.104s
APNP	0.05	0.001	0.5	64	2	-	-	-	-	-	92	3.59	11.856ms/2.415s	
GPRGNN	0.05	0.001	0.5	256	2	-	-	-	-	-	93.75	2.37		
Texas	SGC-1	0.05	1.00E-03	0	64	-	-	-	-	-	-	83.28	5.43	2.55ms/0.54s
	SGC-2	0.01	1.00E-03	0	64	-	-	-	-	-	-	81.31	3.3	2.61ms/0.53s
	GCN	0.05	1.00E-02	0.9	64	2	-	-	-	-	-	83.11	3.2	3.59ms/0.73s
	Snowball-2	0.05	1.00E-02	0.9	64	2	-	-	-	-	-	83.11	3.2	3.98ms/0.82s
	Snowball-3	0.05	1.00E-02	0.9	64	3	-	-	-	-	-	83.11	3.2	5.56ms/1.12s
	GCNII	0.01	1.00E-04	0.5	64	4	-	-	-	1.5	0.5	82.46	4.58	
	GCNII*	0.01	1.00E-04	0.5	64	8	-	-	-	0.5	0.5	88.52	3.02	15.64ms/3.47s
	FAGCN	0.01	5.00E-04	0	32	2	-	-	-	-	-	88.85	4.39	8.8ms/6.5252s
	Mixhop	0.01	0.001	0.5	32	2	-	-	-	-	-	76.39	7.66	11.099ms/2.329s
	H2GCN	0.01	0.001	0.5	64	1	-	-	-	-	-	85.90	3.53	4.197ms/0.95s
	GCN+JK	0.1	0.001	0.5	32	2	-	-	cat	-	-	80.66	1.91	5.28ms/1.085s
	GAT+JK	0.1	0.001	0.5	8	2	2	cat	-	-	-	75.41	7.18	10.937ms/2.402s
Film	SGC-1	0.01	5.00E-06	0	64	-	-	-	-	-	-	25.26	1.18	3.18ms/0.70s
	SGC-2	0.01	5.00E-06	0	64	-	-	-	-	-	-	28.81	1.11	2.13ms/0.43s
	GCN	0.1	5.00E-04	0	64	2	-	-	-	-	-	35.51	0.99	4.86ms/0.99s
	Snowball-2	0.1	5.00E-04	0	64	2	-	-	-	-	-	35.97	0.66	5.59ms/1.14s
	Snowball-3	0.1	5.00E-04	0.2	64	3	-	-	-	-	-	36	1.36	7.89ms/1.60s
	GCNII	0.01	1.00E-04	0.5	64	8	-	-	-	1.5	0.3	40.82	1.79	15.85ms/3.22s
	GCNII*	0.01	1.00E-06	0.5	64	4	-	-	-	1	0.1	41.54	0.99	
	FAGCN	0.01	5.00E-05	0.6	32	2	-	-	-	-	-	31.59	1.37	45.4ms/11.107s
	Mixhop	0.01	0.001	0.5	8	3	8	max	-	-	-	33.13	2.40	17.651ms/3.566s
	H2GCN	0.01	0.001	0	64	1	8	max	-	-	-	38.85	1.17	8.101ms/1.695s
	GCN+JK	0.1	0.001	0.5	64	2	8	cat	-	-	-	32.72	2.62	8.946ms/1.807s
	GAT+JK	0.001	0.001	0.5	32	2	4	cat	-	-	-	35.41	0.97	20.726ms/4.187s
Chameleon	SGC-1	0.1	5.00E-06	0	64	-	-	-	-	-	-	64.86	1.81	3.48ms/2.96s
	SGC-2	0.1	0.00E+00	0	64	-	-	-	-	-	-	62.67	2.41	4.43ms/1.12s
	GCN	0.01	1.00E-05	0.9	64	2	-	-	-	-	-	64.18	2.62	4.96ms/1.18s
	Snowball-2	1.00E-01	1.00E-05	0.9	64	2	-	-	-	-	-	64.99	2.39	4.96ms/1.00s
	Snowball-3	0.1	5.00E-06	0.9	64	3	-	-	-	-	-	65.49	1.64	7.44ms/1.50s
	GCNII	0.01	5.00E-06	0.5	64	4	-	-	-	0.5	0.1	60.35	2.7	9.76ms/2.26s
	GCNII*	0.01	5.00E-04	0.5	64	4	-	-	-	1.5	0.5	62.8	2.17	10.40ms/2.17s
	FAGCN	0.002	1.00E-04	0	32	2	-	-	-	-	-	49.47	2.84	8.4ms/13.8696s
	Mixhop	0.01	0.001	0.5	16	2	8	max	-	-	-	36.28	10.2	11.372ms/2.297s
	H2GCN	0.01	0.001	0	32	1	8	max	-	-	-	52.3	0.48	4.059ms/0.82s
	GCN+JK	0.001	0.001	0.5	32	2	8	cat	-	-	-	64.68	2.85	5.211ms/1.053s
	GAT+JK	0.001	0.001	0.5	4	2	8	max	-	-	-	68.14	1.18	13.772ms/2.788s
Squirrel	SGC-1	0.05	0.00E+00	0	64	-	-	-	-	-	-	47.62	1.27	4.65ms/1.44s
	SGC-2	0.1	0.00E+00	0.9	64	-	-	-	-	-	-	41.25	1.4	35.00ms/7.81s
	GCN	0.01	5.00E-05	0.7	64	2	-	-	-	-	-	44.76	1.39	8.41ms/2.50s
	Snowball-2	0.1	0.00E+00	0.9	64	2	-	-	-	-	-	47.88	1.23	8.96ms/1.92s
	Snowball-3	0.1	0.00E+00	0.8	64	3	-	-	-	-	-	48.25	0.94	14.00ms/2.90s
	GCNII	0.01	1.00E-04	0.5	64	4	-	-	-	1.5	0.2	38.81	1.97	13.35ms/2.70s
	GCNII*	0.01	5.00E-04	0.5	64	4	-	-	-	1.5	0.3	38.31	1.3	13.81ms/2.78s
	FAGCN	0.05	1.00E-04	0	32	2	-	-	-	-	-	42.24	1.2	16ms/6.7961s
	Mixhop	0.01	0.001	0.5	32	2	-	-	-	-	-	24.55	2.6	17.634ms/3.562s
	H2GCN	0.01	0.001	0	16	1	-	-	-	-	-	30.39	1.22	9.315ms/1.882s
	GCN+JK	0.001	0.001	0.5	32	2	-	-	max	-	-	53.4	1.9	14.321ms/2.905s
	GAT+JK	0.001	0.001	0.5	8	2	4	max	-	-	-	52.28	3.61	29.097ms/5.878s
Cora	SGC-1	0.1	5.00E-06	0	64	-	-	-	-	-	-	85.12	1.64	3.47ms/1.55s
	SGC-2	0.1	1.00E-05	0	64	-	-	-	-	-	-	85.48	1.48	2.91ms/6.85s
	GCN	0.1	5.00E-04	0.2	64	2	-	-	-	-	-	87.78	0.96	4.24ms/0.86s
	Snowball-2	0.1	5.00E-04	0.1	64	2	-	-	-	-	-	88.64	1.15	4.65ms/0.94s
	Snowball-3	0.05	1.00E-03	0.6	64	3	-	-	-	-	-	89.33	1.3	6.41ms/1.32s
	GCNII	0.01	1.00E-04	0.5	64	16	-	-	-	0.5	0.2	88.98	1.33	
	GCNII*	0.01	5.00E-04	0.5	64	4	-	-	-	0.5	0.5	88.93	1.37	10.16ms/2.24s
	FAGCN	0.05	5.00E-04	0	32	2	-	-	-	-	-	88.85	1.36	8.4ms/3.3183s
	Mixhop	0.01	0.001	0.5	16	2	-	-	-	-	-	65.65	11.31	11.177ms/2.278s
	H2GCN	0.01	0.001	0	32	1	-	-	-	-	-	87.52	0.61	4.335ms/1.209s
	GCN+JK	0.001	0.001	0.5	64	2	-	-	cat	-	-	86.90	1.51	6.656ms/1.346s
	GAT+JK	0.001	0.001	0.5	32	2	2	cat	-	-	-	89.52	0.43	12.91ms/2.608s
CiteSeer	SGC-1	0.1	5.00E-04	0	64	-	-	-	-	-	-	79.66	0.75	3.43ms/7.30s
	SGC-2	0.01	5.00E-04	0.9	64	-	-	-	-	-	-	80.75	1.15	5.33ms/4.40s
	GCN	0.1	1.00E-03	0.9	64	2	-	-	-	-	-	81.39	1.23	4.18ms/0.86s
	Snowball-2	0.1	1.00E-03	0.8	64	2	-	-	-	-	-	81.53	1.71	5.19ms/1.11s
	Snowball-3	0.1	1.00E-03	0.9	64	3	-	-	-	-	-	80.93	1.32	7.64ms/1.69s
	GCNII	0.01	1.00E-03	0.5	64	16	-	-	-	0.5	0.2	81.58</		

Hyperparameters for ACM-GNNs and ACMII-GNNs														
Datasets	Models/Hyperparameters	lr	weight_decay	dropout	hidden	# layers	Gat heads	JK Type	lambda	alpha_l	results	std	average epoch time/average total time	
Cornell	ACM-SGC-1	0.01	5.00E-03	0.6	64	-	-	-	-	-	93.77	1.91	5.53ms/2.31s	
	ACM-SGC-2	0.01	5.00E-03	0.6	64	-	-	-	-	-	93.77	2.17	4.73ms/1.87s	
	ACM-GCN	0.05	1.00E-02	0.2	64	2	-	-	-	-	94.75	3.8	8.25ms/1.69s	
	ACMII-GCN	0.1	1.00E-02	0.5	64	2	-	-	-	-	95.25	2.79	8.43ms/1.71s	
	ACM-GCNII	0.01	1.00E-03	0.5	64	1	-	-	0.5	0.4	92.62	3.13	6.81ms/1.43s	
	ACM-GCNII*	0.01	5.00E-04	0.5	64	1	-	-	0.5	0.1	93.44	2.74	6.76ms/1.39s	
	ACM-Snowball-2	0.05	1.00E-02	0.2	64	2	-	-	-	-	95.08	3.11	9.15ms/1.86s	
	ACM-Snowball-3	0.1	1.00E-02	0.4	64	3	-	-	-	-	94.26	2.57	13.20ms/2.68s	
	ACMII-Snowball-2	0.05	1.00E-02	0.6	64	2	-	-	-	-	95.25	1.55	8.23ms/1.72s	
ACMII-Snowball-3	0.05	1.00E-02	0.7	64	3	-	-	-	-	93.61	2.79	11.70ms/2.37s		
Wisconsin	ACM-SGC-1	0.05	5.00E-03	0.7	64	-	-	-	-	-	93.25	2.92	5.96ms/1.34s	
	ACM-SGC-2	0.1	5.00E-03	0.2	64	-	-	-	-	-	94	2.61	4.60ms/0.95s	
	ACM-GCN	0.1	5.00E-03	0	64	2	-	-	-	-	95.75	2.03	8.11ms/1.64s	
	ACMII-GCN	0.1	1.00E-02	0.2	64	2	-	-	-	-	96.62	2.44	8.28ms/1.68s	
	ACM-GCNII	0.01	5.00E-03	0.5	64	1	-	-	1	0.1	94.63	2.96	9.31ms/2.19s	
	ACM-GCNII*	0.01	1.00E-03	0.5	64	1	-	-	1.5	0.4	94.37	2.81	7.11ms/1.45s	
	ACM-Snowball-2	0.1	5.00E-03	0.1	64	2	-	-	-	-	96.38	2.59	8.63ms/1.74s	
	ACM-Snowball-3	0.05	1.00E-02	0.3	64	3	-	-	-	-	96.62	1.86	12.79ms/2.58s	
	ACMII-Snowball-2	0.1	1.00E-02	0.1	64	2	-	-	-	-	96.63	2.24	8.11ms/1.65s	
ACMII-Snowball-3	0.1	5.00E-03	0.1	64	3	-	-	-	-	97	2.63	12.38ms/2.51s		
Texas	ACM-SGC-1	0.01	5.00E-03	0.6	64	-	-	-	-	-	93.61	1.55	5.43ms/2.18s	
	ACM-SGC-2	0.05	5.00E-03	0.4	64	-	-	-	-	-	93.44	2.54	4.59ms/1.01s	
	ACM-GCN	0.05	1.00E-02	0.6	64	2	-	-	-	-	94.92	2.88	8.33ms/1.70s	
	ACMII-GCN	0.1	5.00E-03	0.4	64	2	-	-	-	-	95.08	2.54	8.49ms/1.72s	
	ACM-GCNII	0.01	1.00E-03	0.5	64	1	-	-	0.5	0.4	92.46	1.97	6.47ms/1.36s	
	ACM-GCNII*	0.01	1.00E-03	0.5	64	1	-	-	0.5	0.4	93.28	2.79	7.03ms/1.45s	
	ACM-Snowball-2	0.05	1.00E-02	0.1	64	2	-	-	-	-	95.74	2.22	8.35ms/1.71s	
	ACM-Snowball-3	0.01	5.00E-03	0.6	64	3	-	-	-	-	94.75	2.41	12.56ms/2.63s	
	ACMII-Snowball-2	0.1	1.00E-02	0.4	64	2	-	-	-	-	95.25	1.55	9.74ms/1.97s	
ACMII-Snowball-3	0.05	1.00E-02	0.6	64	3	-	-	-	-	94.75	3.09	11.91ms/2.42s		
Film	ACM-SGC-1	0.05	5.00E-05	0.7	64	-	-	-	-	-	39.33	1.25	5.21ms/2.33s	
	ACM-SGC-2	0.1	5.00E-05	0.7	64	-	-	-	-	-	40.13	1.21	12.41ms/4.87s	
	ACM-GCN	0.1	5.00E-04	0.5	64	2	-	-	-	-	41.62	1.15	10.72ms/2.66s	
	ACMII-GCN	0.1	5.00E-04	0.5	64	2	-	-	-	-	41.24	1.16	10.51ms/2.44s	
	ACM-GCNII	0.01	0.00E+00	0.5	64	3	-	-	1.5	0.2	41.37	1.37	13.65ms/2.74s	
	ACM-GCNII*	0.01	1.00E-05	0.5	64	3	-	-	1.5	0.1	41.27	1.24	14.98ms/3.01s	
	ACM-Snowball-2	0.1	5.00E-03	0	64	2	-	-	-	-	41.4	1.23	10.30ms/2.08s	
	ACM-Snowball-3	0.05	1.00E-02	0	64	3	-	-	-	-	41.27	0.8	16.43ms/3.52s	
	ACMII-Snowball-2	0.1	5.00E-03	0	64	2	-	-	-	-	41.1	0.75	10.74ms/2.19s	
ACMII-Snowball-3	0.05	5.00E-03	0.2	64	3	-	-	-	-	40.31	1.6	16.31ms/3.29s		
Chameleon	ACM-SGC-1	0.1	5.00E-06	0.9	64	-	-	-	-	-	63.68	1.62	5.41ms/1.21s	
	ACM-SGC-2	0.1	5.00E-06	0.9	64	-	-	-	-	-	60.48	1.55	7.86ms/1.81s	
	ACM-GCN	0.01	5.00E-05	0.8	64	2	-	-	-	-	68.18	1.67	10.55ms/3.12s	
	ACMII-GCN	0.05	5.00E-05	0.7	64	2	-	-	-	-	68.38	1.36	10.90ms/2.39s	
	ACM-GCNII	0.01	5.00E-06	0.5	64	4	-	-	0.5	0.1	58.73	2.52	18.31ms/3.68s	
	ACM-GCNII*	0.01	1.00E-03	0.5	64	1	-	-	1	0.1	61.66	2.29	6.68ms/1.40s	
	ACM-Snowball-2	0.05	5.00E-05	0.7	64	2	-	-	-	-	68.51	1.7	9.92ms/2.06s	
	ACM-Snowball-3	0.01	1.00E-04	0.7	64	3	-	-	-	-	68.4	2.05	14.49ms/3.15s	
	ACMII-Snowball-2	0.1	5.00E-05	0.6	64	2	-	-	-	-	67.83	2.63	9.99ms/2.10s	
ACMII-Snowball-3	0.05	1.00E-04	0.7	64	3	-	-	-	-	67.53	2.83	15.03ms/3.29s		
Squirrel	ACM-SGC-1	0.05	0.00E+00	0.9	64	-	-	-	-	-	46.4	1.13	6.96ms/2.16s	
	ACM-SGC-2	0.05	0.00E+00	0.9	64	-	-	-	-	-	40.91	1.39	35.20ms/10.66s	
	ACM-GCN	0.05	5.00E-06	0.6	64	2	-	-	-	-	58.02	1.86	14.35ms/2.98s	
	ACMII-GCN	0.05	0.00E+00	0.7	64	2	-	-	-	-	53.76	1.63	14.08ms/3.39s	
	ACM-GCNII	0.01	1.00E-05	0.5	64	4	-	-	0.5	0.1	40.9	1.58	20.72ms/4.17s	
	ACM-GCNII*	0.01	1.00E-03	0.5	64	4	-	-	0.5	0.3	38.32	1.5	21.78ms/4.38s	
	ACM-Snowball-2	0.05	5.00E-06	0.6	64	2	-	-	-	-	55.97	2.03	15.38ms/3.15s	
	ACM-Snowball-3	0.01	1.00E-04	0.6	64	3	-	-	-	-	55.73	2.39	26.15ms/5.94s	
	ACMII-Snowball-2	0.1	5.00E-06	0.6	64	2	-	-	-	-	53.48	0.6	15.54ms/3.19s	
ACMII-Snowball-3	0.05	5.00E-05	0.5	64	3	-	-	-	-	52.31	1.57	26.24ms/5.30s		
Cora	ACM-SGC-1	0.01	5.00E-06	0.9	64	-	-	-	-	-	86.63	1.13	6.00ms/7.40s	
	ACM-SGC-2	0.1	5.00E-05	0.6	64	-	-	-	-	-	87.64	0.99	4.85ms/1.17s	
	ACM-GCN	0.1	5.00E-03	0.5	64	2	-	-	-	-	88.62	1.22	8.84ms/1.81s	
	ACMII-GCN	0.1	5.00E-03	0.4	64	2	-	-	-	-	89	0.72	8.93ms/1.83s	
	ACM-GCNII	0.01	1.00E-03	0.5	64	3	-	-	1	0.2	89.1	1.61	14.07ms/3.04s	
	ACM-GCNII*	0.01	1.00E-02	0.5	64	4	-	-	1	0.2	89	1.35	11.36ms/2.48s	
	ACM-Snowball-2	0.05	1.00E-03	0.6	64	2	-	-	-	-	88.83	1.49	9.34ms/1.92s	
	ACM-Snowball-3	0.1	1.00E-02	0.3	64	3	-	-	-	-	89.59	1.58	13.33ms/2.75s	
	ACMII-Snowball-2	0.1	5.00E-03	0.5	64	2	-	-	-	-	88.95	1.04	9.29ms/1.90s	
ACMII-Snowball-3	0.1	5.00E-03	0.5	64	3	-	-	-	-	89.36	1.26	14.18ms/2.89s		
CiteSeer	ACM-SGC-1	0.01	5.00E-04	0.9	64	-	-	-	-	-	80.96	0.93	5.90ms/4.31s	
	ACM-SGC-2	0.05	5.00E-04	0.9	64	-	-	-	-	-	80.93	1.16	5.01ms/1.42s	
	ACM-GCN	0.05	5.00E-03	0.7	64	2	-	-	-	-	81.68	0.97	11.35ms/2.57s	
	ACMII-GCN	0.05	5.00E-05	0.7	64	2	-	-	-	-	81.58	1.77	9.55ms/1.94s	
	ACM-GCNII	0.01	1.00E-02	0.5	64	3	-	-	0.5	0.3	82.28	1.12	15.61ms/3.56s	
	ACM-GCNII*	0.01	1.00E-02	0.5	64	3	-	-	0.5	0.5	81.69	1.25	15.56ms/3.61s	
	ACM-Snowball-2	0.05	5.00E-03	0.7	64	2	-	-	-	-	81.58	1.23	11.14ms/2.50s	
	ACM-Snowball-3	0.01	5.00E-03	0.9	64	3	-	-	-	-	81.32	0.97	15.91ms/3.56s	
	ACMII-Snowball-2	0.05	5.00E-03	0.7	64	2	-	-	-	-	82.07	1.04	10.97ms/2.55s	
ACMII-Snowball-3	0.05	1.00E-04	0.6	64	3	-	-	-	-	81.56	1.15	14.95ms/3.03s		
PubMed	ACM-SGC-1	0.05	5.00E-06	0.3	64	-	-	-	-	-	87.75	0.88	6.04ms/2.61s	
	ACM-SGC-2	0.05	5.00E-05	0.1	64	-	-	-	-	-	88.79	0.5	8.62ms/3.18s	
	ACM-GCN	0.1	5.00E-04	0.2	64	2	-	-	-	-	90.54	0.63	10.20ms/2.08s	
	ACMII-GCN	0.1	5.00E-04	0.2	64	2	-	-	-	-	90.74	0.5	10.20ms/2.07s	
	ACM-GCNII	0.01	1.00E-04	0.5	64	3	-	-	1.5	0.5	90.12	0.4	15.07ms/3.35s	
	ACM-GCNII*	0.01	1.00E-04	0.5	64	3	-	-	1.5	0.5	90.18	0.51	16.62ms/3.72s	
	ACM-Snowball-2	0.1	1.00E-04	0.3	64	2	-	-	-	-	90.81	0.52	11.52ms/2.36s	
	ACM-Snowball-3	0.05	1.00E-03	0.2	64	3	-	-	-	-	91.44	0.59	18.06ms/3.69s	
	ACMII-Snowball-2	0.1	1.00E-04	0.3	64	2	-	-	-	-	90.56	0.39	11.74ms/2.39s	
ACMII-Snowball-3	0.1	5.00E-04	0.2	64	3	-	-	-	-	91.31	0.6	18.61ms/3.88s		
Deezer-Europe	ACM-SGC-1	0.05	0.5e-6,1e-5,5e-5	0.3	64	-	-	-	-	-	66.67	0.56	146.41ms/73.06s	
	ACM-SGC-2	0.002	5e-5,1e-4	0.3	64	-	-	-	-	-	66.53	0.57	195.21ms/97.41s	
	ACM-GCN	0.002	5.00E-04	0.5	64	2	-	-	-	-	67.01	0.38	136.45ms/68.09s	
	ACMII-GCN	0.01	5.00E-05	0.8	64	2	-	-	-	-	67.15	0.41	135.24ms/67.48s	
	ACM-GCNII	0.01	0.5e-6	0.5	64	1	-	-	0.5	0.4	66.39	0.56	80.82ms/40.33s	
	ACM-GCNII*	0.01	0.0001,1e-3	0.5	64	1	-	-	1.5	0.2	66.6	0.57	80.95ms/40.40s	

Table 7: Hyperparameters for ACM-GNNs and ACMII-GNNs

B Details of Gradient Calculation in (5)

B.1 Derivation in Matrix Form

In output layer, we have

$$Y = \text{softmax}(\hat{A}XW) \equiv \text{softmax}(Y') = (\exp(Y')\mathbf{1}_C\mathbf{1}_C^T)^{-1} \odot \exp(Y') > 0$$

$$\mathcal{L} = -\text{trace}(Z^T \log Y)$$

where $\mathbf{1}_C \in \mathcal{R}^{C \times 1}$, $(\cdot)^{-1}$ is point-wise inverse function and each element of Y is positive. Then

$$d\mathcal{L} = -\text{trace}(Z^T((Y)^{-1} \odot dY)) = -\text{trace}\left(Z^T \left((\text{softmax}(Y'))^{-1} \odot d \text{softmax}(Y') \right)\right)$$

Note that

$$\begin{aligned} d \text{softmax}(Y') &= -(\exp(Y')\mathbf{1}_C\mathbf{1}_C^T)^{-2} \odot [(\exp(Y') \odot dY')\mathbf{1}_C\mathbf{1}_C^T] \odot \exp(Y') \\ &\quad + (\exp(Y')\mathbf{1}_C\mathbf{1}_C^T)^{-1} \odot (\exp(Y') \odot dY') \\ &= -\text{softmax}(Y') \odot (\exp(Y')\mathbf{1}_C\mathbf{1}_C^T)^{-1} \odot [(\exp(Y') \odot dY')\mathbf{1}_C\mathbf{1}_C^T] \\ &\quad + \text{softmax}(Y') \odot dY' \\ &= \text{softmax}(Y') \odot \left(-(\exp(Y')\mathbf{1}_C\mathbf{1}_C^T)^{-1} \odot [(\exp(Y') \odot dY')\mathbf{1}_C\mathbf{1}_C^T] + dY' \right) \end{aligned}$$

Then,

$$\begin{aligned} d\mathcal{L} &= -\text{trace}\left(Z^T \left((\text{softmax}(Y'))^{-1} \odot \left[\text{softmax}(Y') \odot \left(-(\exp(Y')\mathbf{1}_C\mathbf{1}_C^T)^{-1} \right. \right. \right. \right. \\ &\quad \left. \left. \left. \odot [(\exp(Y') \odot dY')\mathbf{1}_C\mathbf{1}_C^T] + dY' \right) \right] \right)\right) \\ &= -\text{trace}\left(Z^T \left(-(\exp(Y')\mathbf{1}_C\mathbf{1}_C^T)^{-1} \odot [(\exp(Y') \odot dY')\mathbf{1}_C\mathbf{1}_C^T] + dY' \right)\right) \\ &= \text{trace}\left(\left((Z \odot (\exp(Y')\mathbf{1}_C\mathbf{1}_C^T)^{-1}) \mathbf{1}_C\mathbf{1}_C^T \right)^T [\exp(Y') \odot dY'] - Z^T dY' \right) \\ &= \text{trace}\left(\left(\exp(Y') \odot \left((Z \odot (\exp(Y')\mathbf{1}_C\mathbf{1}_C^T)^{-1}) \mathbf{1}_C\mathbf{1}_C^T \right) \right)^T dY' - Z^T dY' \right) \\ &= \text{trace}\left(\left(\exp(Y') \odot (\exp(Y')\mathbf{1}_C\mathbf{1}_C^T)^{-1} \right)^T dY' - Z^T dY' \right) \\ &= \text{trace}((\text{softmax}(Y') - Z)^T dY') \end{aligned}$$

where the 4-th equation holds due to $(Z \odot (\exp(Y')\mathbf{1}_C\mathbf{1}_C^T)^{-1}) \mathbf{1}_C\mathbf{1}_C^T = (\exp(Y')\mathbf{1}_C\mathbf{1}_C^T)^{-1}$. Thus, we have

$$\frac{d\mathcal{L}}{dY'} = \text{softmax}(Y') - Z = Y - Z$$

For Y' and W , we have

$$dY' = \hat{A}X dW \text{ and } d\mathcal{L} = \text{trace}\left(\frac{d\mathcal{L}}{dY'}^T dY'\right) = \text{trace}\left(\frac{d\mathcal{L}}{dY'}^T \hat{A}X dW\right) = \text{trace}\left(\frac{d\mathcal{L}}{dW}^T dW\right)$$

To get $\frac{d\mathcal{L}}{dW}$ we have,

$$\frac{d\mathcal{L}}{dW} = X^T \hat{A}^T \frac{d\mathcal{L}}{dY'} = X^T \hat{A}^T (Y - Z) \quad (14)$$

B.2 Component-wise Derivation

Denote $\tilde{X} = XW$. We rewrite \mathcal{L} as follows:

$$\begin{aligned}
\mathcal{L} &= -\text{trace} \left(Z^T \log \left((\exp(Y') \mathbf{1}_C \mathbf{1}_C^T)^{-1} \odot \exp(Y') \right) \right) \\
&= -\text{trace} \left(Z^T \left(-\log(\exp(Y') \mathbf{1}_C \mathbf{1}_C^T) + Y' \right) \right) \\
&= -\text{trace} \left(Z^T Y' \right) + \text{trace} \left(Z^T \log \left(\exp(Y') \mathbf{1}_C \mathbf{1}_C^T \right) \right) \\
&= -\text{trace} \left(Z^T \hat{A} X W \right) + \text{trace} \left(Z^T \log \left(\exp(Y') \mathbf{1}_C \mathbf{1}_C^T \right) \right) \\
&= -\text{trace} \left(Z^T \hat{A} X W \right) + \text{trace} \left(\mathbf{1}_C^T \log \left(\exp(Y') \mathbf{1}_C \right) \right) \\
&= -\sum_{i=1}^N \sum_{j \in \mathcal{N}_i} \hat{A}_{i,j} Z_{i,:} \tilde{X}_{j,:}^T + \sum_{i=1}^N \log \left(\sum_{c=1}^C \exp \left(\sum_{j \in \mathcal{N}_i} \hat{A}_{i,j} \tilde{X}_{j,c} \right) \right) \\
&= -\sum_{i=1}^N \log \left(\exp \left(\sum_{c=1}^C \sum_{j \in \mathcal{N}_i} \hat{A}_{i,j} Z_{i,c} \tilde{X}_{j,c} \right) \right) + \sum_{i=1}^N \log \left(\sum_{c=1}^C \exp \left(\sum_{j \in \mathcal{N}_i} \hat{A}_{i,j} \tilde{X}_{j,c} \right) \right) \\
&= -\sum_{i=1}^N \log \frac{\exp \left(\sum_{c=1}^C \sum_{j \in \mathcal{N}_i} \hat{A}_{i,j} Z_{i,c} \tilde{X}_{j,c} \right)}{\left(\sum_{c=1}^C \exp \left(\sum_{j \in \mathcal{N}_i} \hat{A}_{i,j} \tilde{X}_{j,c} \right) \right)}
\end{aligned}$$

Note that $\sum_{c=1}^C Z_{j,c} = 1$ for any j . Consider the derivation of \mathcal{L} over $\tilde{X}_{j',c'}$:

$$\begin{aligned}
&\frac{d\mathcal{L}}{d\tilde{X}_{j',c'}} \\
&= -\sum_{i=1}^N \frac{\sum_{c=1}^C \exp \left(\sum_{j \in \mathcal{N}_i} \hat{A}_{i,j} \tilde{X}_{j,c} \right)}{\exp \left(\sum_{c=1}^C \sum_{j \in \mathcal{N}_i} \hat{A}_{i,j} Z_{i,c} \tilde{X}_{j,c} \right)} \\
&\quad \times \left(\frac{\left(\hat{A}_{i,j'} Z_{i,c'} \right) \exp \left(\sum_{c=1}^C \sum_{j \in \mathcal{N}_i} \hat{A}_{i,j} Z_{i,c} \tilde{X}_{j,c} \right) \left(\sum_{c=1}^C \exp \left(\sum_{j \in \mathcal{N}_i} \hat{A}_{i,j} \tilde{X}_{j,c} \right) \right)}{\left(\sum_{c=1}^C \exp \left(\sum_{j \in \mathcal{N}_i} \hat{A}_{i,j} \tilde{X}_{j,c} \right) \right)^2} \right. \\
&\quad \left. - \frac{\left(\hat{A}_{i,j'} \right) \exp \left(\sum_{c=1}^C \sum_{j \in \mathcal{N}_i} \hat{A}_{i,j} Z_{i,c} \tilde{X}_{j,c} \right) \left(\exp \left(\sum_{j \in \mathcal{N}_i} \hat{A}_{i,j} \tilde{X}_{j,c'} \right) \right)}{\left(\sum_{c=1}^C \exp \left(\sum_{j \in \mathcal{N}_i} \hat{A}_{i,j} \tilde{X}_{j,c} \right) \right)^2} \right) \\
&= -\sum_{i=1}^N \left(\frac{\left(\hat{A}_{i,j'} Z_{i,c'} \right) \left(\sum_{c=1}^C \exp \left(\sum_{j \in \mathcal{N}_i} \hat{A}_{i,j} \tilde{X}_{j,c} \right) \right) - \left(\hat{A}_{i,j'} \right) \left(\exp \left(\sum_{j \in \mathcal{N}_i} \hat{A}_{i,j} \tilde{X}_{j,c'} \right) \right)}{\left(\sum_{c=1}^C \exp \left(\sum_{j \in \mathcal{N}_i} \hat{A}_{i,j} \tilde{X}_{j,c} \right) \right)} \right)
\end{aligned}$$

$$\begin{aligned}
&= - \sum_{i=1}^N \left(\hat{A}_{i,j'} \frac{\left(\sum_{c=1, c \neq c'}^C (Z_{i,c'}) \exp\left(\sum_{j \in \mathcal{N}_i} \hat{A}_{i,j} \tilde{X}_{j,c} \right) \right) + (Z_{i,c'} - 1) \left(\exp\left(\sum_{j \in \mathcal{N}_i} \hat{A}_{i,j} \tilde{X}_{j,c'} \right) \right)}{\left(\sum_{c=1}^C \exp\left(\sum_{j \in \mathcal{N}_i} \hat{A}_{i,j} \tilde{X}_{j,c} \right) \right)} \right) \\
&= - \sum_{i=1}^N \hat{A}_{i,j'} \left(Z_{i,c'} \hat{P}(Y_i \neq c') + (Z_{i,c'} - 1) \hat{P}(Y_i = c') \right) \\
&= - \sum_{i=1}^N \hat{A}_{i,j'} \left(Z_{i,c'} - \hat{P}(Y_i = c') \right)
\end{aligned}$$

Writing the above in matrix form, we have

$$\frac{d\mathcal{L}}{d\tilde{X}} = \hat{A}(Z - Y), \quad \frac{d\mathcal{L}}{d\tilde{W}} = X^T \hat{A}^T (Z - Y), \quad \Delta Y' \propto \hat{A} X X^T \hat{A}^T (Z - Y) \quad (15)$$

C Details of Synthetic Experiments

In our synthetic experiments, we generate graphs with edge homophily levels $h \in 0.95 : 0.05 : 0.05$ and $h \in 0.05 : 0.005 : 0.005$. We explore the interval $[0.05, 0.005]$ with a more fine-grained scale 0.005 because we empirically find that the performance of GNNs is sensitive in more this area. For a given h , we generate intra-class edges from `numpy.random.multinomial(2, numpy.ones(399)/399, size=1)[0]` (does not include self-loop) and inter-class edges from `numpy.random.multinomial(int(2/h - 2), numpy.ones(1600)/1600, size=1)[0]`.

D Proof of Theorem 1

Proof. According to the given assumptions, for node v , we have $\hat{A}_{v,k} = \frac{1}{d+1}$, the expected number of intra-class edges is dh (here the self-loop edge introduced by \hat{A} is not counted based on the definition of edge homophily and data generation process) and inter-class edges is $(1-h)d$. Suppose there are $C \geq 2$ classes. Consider matrix $\hat{A}Z$,

Then, we have $\mathbb{E} \left[(\hat{A}Z)_{v,c} \right] = \mathbb{E} \left[\sum_{k \in \mathcal{V}} \hat{A}_{v,k} \mathbf{1}_{\{Z_{k,:} = e_c^T\}} \right] = \sum_{k \in \mathcal{V}} \frac{\mathbb{E}[\mathbf{1}_{\{Z_{k,:} = e_c^T\}}]}{d+1}$, where $\mathbf{1}$ is the indicator function.

When v is in class c , we have $\sum_{k \in \mathcal{V}} \frac{\mathbb{E}[\mathbf{1}_{\{Z_{k,:} = e_c^T\}}]}{d+1} = \frac{hd+1}{d+1}$ ($hd+1 = hd$ intra-class edges + 1 self-loop introduced by \hat{A}).

When v is not in class c , we have $\sum_{k \in \mathcal{V}} \frac{\mathbb{E}[\mathbf{1}_{\{Z_{k,:} = e_c^T\}}]}{d+1} = \frac{(1-h)d}{(C-1)(d+1)}$ ($(1-h)d$ inter-class edges uniformly distributed in the other $C-1$ classes).

For nodes v, u , we have $(\hat{A}Z)_{v,:}, (\hat{A}Z)_{u,:} \in \mathbb{R}^C$ and since elements in $\hat{A}_{v,k}$ and $\hat{A}_{u,k'}$ are independently generated for all $k, k' \in \mathcal{V}$, we have

$$\begin{aligned}
\mathbb{E} \left[(\hat{A}Z)_{v,c} (\hat{A}Z)_{u,c} \right] &= \mathbb{E} \left[\left(\sum_{k \in \mathcal{V}} \hat{A}_{v,k} \mathbf{1}_{\{Z_{k,:} = e_c^T\}} \right) \left(\sum_{k' \in \mathcal{V}} \hat{A}_{u,k'} \mathbf{1}_{\{Z_{k',:} = e_c^T\}} \right) \right] \\
&= \mathbb{E} \left[\left(\sum_{k \in \mathcal{V}} \hat{A}_{v,k} \mathbf{1}_{\{Z_{k,:} = e_c^T\}} \right) \right] \mathbb{E} \left[\left(\sum_{k' \in \mathcal{V}} \hat{A}_{u,k'} \mathbf{1}_{\{Z_{k',:} = e_c^T\}} \right) \right]
\end{aligned}$$

Thus,

$$\begin{aligned}\mathbb{E} \left[S(\hat{A}, Z)_{v,u} \right] &= \mathbb{E} \left[\langle (\hat{A}Z)_{v,:}, (\hat{A}Z)_{u,:} \rangle \right] = \sum_c \mathbb{E} \left[\left(\sum_{k \in \mathcal{V}} \hat{A}_{v,k} \mathbf{1}_{\{Z_{k,:} = e_c^T\}} \right) \right] \mathbb{E} \left[\left(\sum_{k' \in \mathcal{V}} \hat{A}_{u,k'} \mathbf{1}_{\{Z_{k',:} = e_c^T\}} \right) \right] \\ &= \begin{cases} \left(\frac{hd+1}{d+1} \right)^2 + \frac{((1-h)d)^2}{(C-1)(d+1)^2}, & u, v \text{ are in the same class} \\ \frac{2(hd+1)(1-h)d}{(C-1)(d+1)^2} + \frac{(C-2)(1-h)^2 d^2}{(C-1)^2(d+1)^2}, & u, v \text{ are in different classes} \end{cases}\end{aligned}$$

For nodes u_1, u_2 , and v , where $Z_{u_1,:} = Z_{v,:}$ and $Z_{u_2,:} \neq Z_{v,:}$,

$$\begin{aligned}g(h) &\equiv \mathbb{E} \left[S(\hat{A}, Z)_{v,u_1} \right] - \mathbb{E} \left[S(\hat{A}, Z)_{v,u_2} \right] \tag{16} \\ &= \frac{(C-1)^2(hd+1)^2 + (C-1)[(1-h)d]^2 - (C-1)(2(hd+1)(1-h)d) - (C-2)[(1-h)d]^2}{(C-1)^2(d+1)^2} \\ &= \left(\frac{(C-1)(hd+1) - (1-h)d}{(C-1)(d+1)} \right)^2\end{aligned}$$

Setting $g(h) = 0$, we obtain the optimal h :

$$h = \frac{d+1-C}{Cd} \tag{17}$$

For the data generation process in the synthetic experiments, we fix d_{intra} , then $d = d_{\text{intra}}/h$, which is a function of h . We change d in (17) to d_{intra}/h , leading to

$$h = \frac{d_{\text{intra}}/h + 1 - C}{Cd_{\text{intra}}/h} \tag{18}$$

It is easy to observe that h satisfying (18) still makes $g(h) = 0$, when d in $g(h)$ is replaced by d_{intra}/h . From (18) we obtain the optimal h in terms of d_{intra} :

$$h = \frac{d_{\text{intra}}}{Cd_{\text{intra}} + C - 1}$$

□

D.1 An extension of Theorem 1

$$\begin{aligned}S_{\text{agg}} \left(S(\hat{A}, Z) \right) &= \frac{\left| \left\{ v \mid \text{Mean}_u(\{S(\hat{A}, Z)_{v,u} \mid Z_{u,:} = Z_{v,:}\}) \geq \text{Mean}_u(\{S(\hat{A}, Z)_{v,u} \mid Z_{u,:} \neq Z_{v,:}\}) \right\} \right|}{|\mathcal{V}|} \\ &= \frac{\sum_{v \in \mathcal{V}} \mathbf{1}_{\left\{ \text{Mean}_u(\{S(\hat{A}, Z)_{v,u} \mid Z_{u,:} = Z_{v,:}\}) \geq \text{Mean}_u(\{S(\hat{A}, Z)_{v,u} \mid Z_{u,:} \neq Z_{v,:}\}) \right\}}}{|\mathcal{V}|}\end{aligned}$$

Then,

$$\begin{aligned}\mathbb{E} \left(S_{\text{agg}} \left(S(\hat{A}, Z) \right) \right) &= \mathbb{E} \left(\frac{\sum_{v \in \mathcal{V}} \mathbf{1}_{\left\{ \text{Mean}_u(\{S(\hat{A}, Z)_{v,u} \mid Z_{u,:} = Z_{v,:}\}) \geq \text{Mean}_u(\{S(\hat{A}, Z)_{v,u} \mid Z_{u,:} \neq Z_{v,:}\}) \right\}}}{|\mathcal{V}|} \right) \\ &= \frac{\sum_{v \in \mathcal{V}} \mathbb{P} \left(\text{Mean}_u(\{S(\hat{A}, Z)_{v,u} \mid Z_{u,:} = Z_{v,:}\}) \geq \text{Mean}_u(\{S(\hat{A}, Z)_{v,u} \mid Z_{u,:} \neq Z_{v,:}\}) \right)}{|\mathcal{V}|} \\ &= \mathbb{P} \left(\text{Mean}_u(\{S(\hat{A}, Z)_{v,u} \mid Z_{u,:} = Z_{v,:}\}) - \text{Mean}_u(\{S(\hat{A}, Z)_{v,u} \mid Z_{u,:} \neq Z_{v,:}\}) \geq 0 \right)\end{aligned}$$

Consider the random variable

$$RV = \text{Mean}_u(\{S(\hat{A}, Z)_{v,u} \mid Z_{u,:} = Z_{v,:}\}) - \text{Mean}_u(\{S(\hat{A}, Z)_{v,u} \mid Z_{u,:} \neq Z_{v,:}\})$$

Since RV is symmetrically distributed and under the conditions in theorem 1, its expectation is $\mathbb{E}[RV] = g(h)$ as showed in (16). Since the minimum of $g(h)$ is 0 and RV is symmetrically distributed, we have $\mathbb{P}(RV \geq 0) \geq 0.5$ and this can explain why $H_{\text{agg}}(\mathcal{G})$ is always greater than 0.5 in many real-world tasks.

E Proof of Theorem 2

Proof. Define $W_v^c = (\hat{A}Z)_{v,c}$. Then,

$$W_v^c = \sum_{k \in \mathcal{V}} \hat{A}_{v,k} \mathbf{1}_{\{Z_{k,:} = e_c^T\}} \in [0, 1], \quad \sum_{c=1}^C W_v^c = 1$$

Note that

$$S(I - \hat{A}, Z) = (I - \hat{A})ZZ^T(I - \hat{A})^T = ZZ^T + \hat{A}ZZ^T\hat{A}^T - \hat{A}ZZ^T - ZZ^T\hat{A}^T \quad (19)$$

For any node v , let the class v belongs to be denoted by c_v . For two nodes v, u , if $Z_{v,:} \neq Z_{u,:}$, we have

$$\begin{aligned} (ZZ^T)_{v,u} &= 0 \\ (\hat{A}ZZ^T\hat{A}^T)_{v,u} &= \sum_{c=1}^C W_v^c W_u^c \\ (\hat{A}ZZ^T)_{v,u} &= W_v^{c_u} \\ (ZZ^T\hat{A}^T)_{v,u} &= (\hat{A}ZZ^T)_{u,v} = W_u^{c_v} \end{aligned}$$

Then, from (19) it follows that

$$(S(I - \hat{A}, Z))_{v,u} = \sum_{c=1}^C W_v^c W_u^c - W_v^{c_u} - W_u^{c_v}$$

When $C = 2$,

$$S(I - \hat{A}, Z)_{v,u} = W_v^{c_u} (W_u^{c_u} - 1) + W_u^{c_v} (W_v^{c_v} - 1) \leq 0$$

If $Z_{v,:} = Z_{u,:}$, i.e., $c_v = c_u$, we have

$$\begin{aligned} (ZZ^T)_{v,u} &= 1 \\ (\hat{A}ZZ^T\hat{A}^T)_{v,u} &= \sum_{c=1}^C W_v^c W_u^c \\ (\hat{A}ZZ^T)_{v,u} &= W_v^{c_v} \\ (ZZ^T\hat{A}^T)_{v,u} &= (\hat{A}ZZ^T)_{u,v} = W_u^{c_u} = W_u^{c_v} \end{aligned}$$

Then, from (19) it follows that

$$\begin{aligned} S(I - \hat{A}, Z)_{v,u} &= 1 + \sum_{c=1}^C W_v^c W_u^c - W_v^{c_v} - W_u^{c_v} \\ &= \sum_{c=1, c \neq c_v}^C W_v^c W_u^c + 1 + W_v^{c_v} W_u^{c_v} - W_v^{c_v} - W_u^{c_v} \\ &= \sum_{c=1, c \neq c_v}^C W_v^c W_u^c + (1 - W_v^{c_v})(1 - W_u^{c_v}) \geq 0 \end{aligned}$$

Thus, if $C = 2$, for any $v \in \mathcal{V}$, if $Z_{u,:} \neq Z_{v,:}$, we have $S(I - \hat{A}, Z)_{v,u} \leq 0$; if $Z_{u,:} = Z_{v,:}$, we have $S(I - \hat{A}, Z)_{v,u} \geq 0$. Apparently, the two conditions in (10) are satisfied. Thus v is diversification distinguishable and $\text{DD}_{\hat{A}, X}(\mathcal{G}) = 1$. The theorem is proved. \square

F Model Comparison on Synthetic Graphs

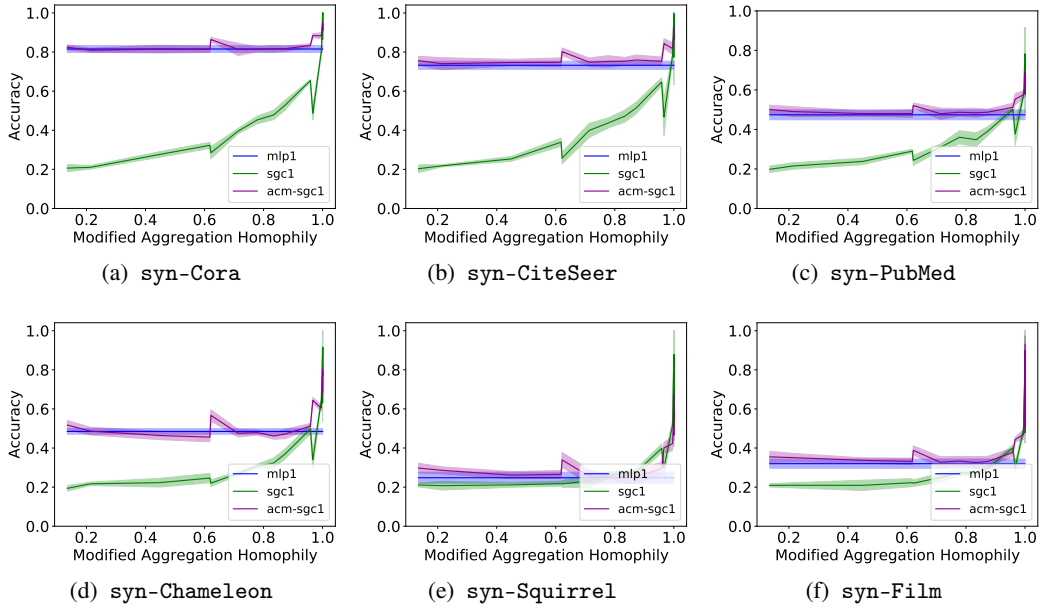


Figure 4: Comparison of test accuracy (mean \pm std) of MLP-1, SGC-1 and ACM-SGC-1 on synthetic datasets

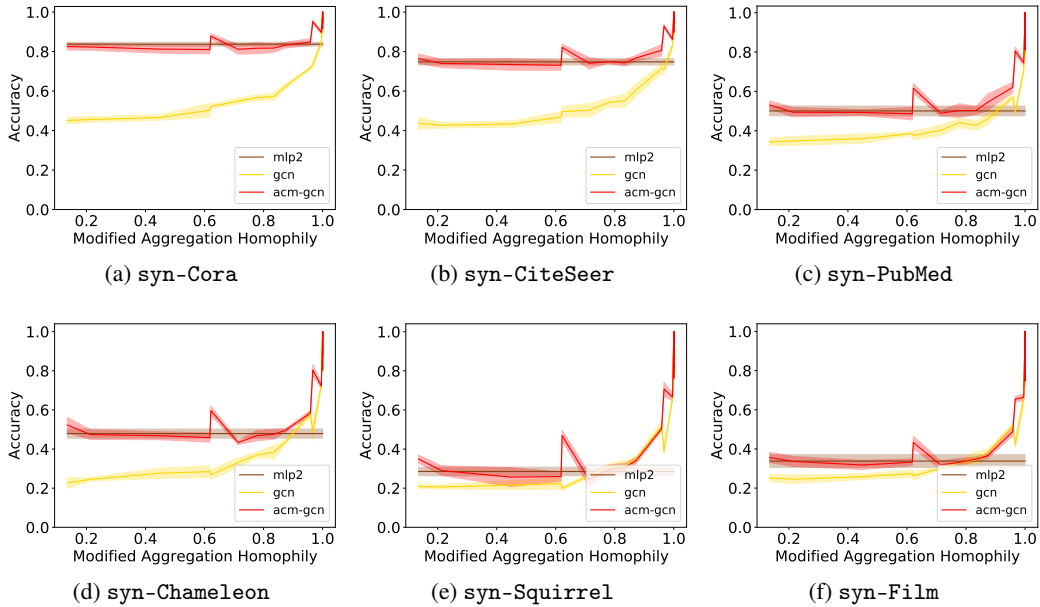


Figure 5: Comparison of test accuracy (mean \pm std) of MLP-2, GCN and ACM-GCN on synthetic datasets

In order to separate the effects of nonlinearity and graph structure, we compare sgc with 1 hop (sgc-1) with MLP-1 (linear model). For GCN which includes nonlinearity, we use MLP-2 as the graph-agnostic baseline model. We train the above GNN models, graph-agnostic baseline models and

ACM-GNN models on all synthetic datasets and plot the mean test accuracy with standard deviation on each dataset. From Figure 4 and Figure 5, we can see that on each $H_{\text{agg}}^M(\mathcal{G})$ level, ACM-GNNs will not underperform GNNs and graph-agnostic models. But when $H_{\text{agg}}^M(\mathcal{G})$ is small, GNNs will be outperformed by graph-agnostic models by a large margin. This demonstrate the advantage of the ACM framework.

G Discussion of the Limitations of Diversification Operation

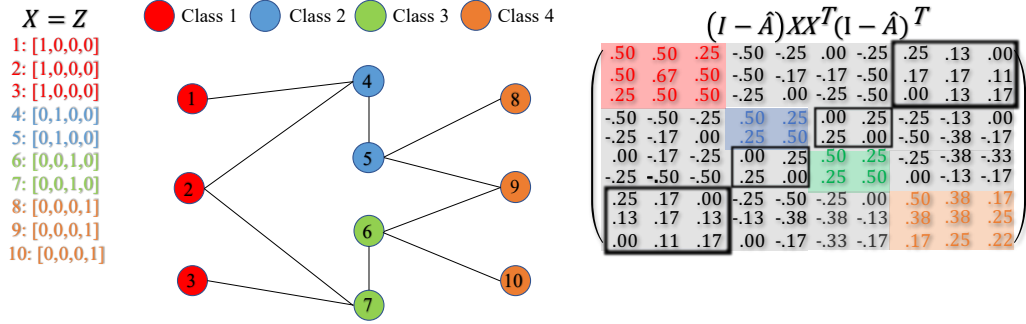


Figure 6: Example of the case (the area in black box) that HP filter does not work well for harmful heterophily

From the black box area of $S(I - \hat{A}, X)$ in the example in Figure 6 we can see that nodes in class 1 and 4 assign non-negative weights to each other; nodes in class 2 and 3 assign non-negative weights to each other as well. This is because the surrounding differences of class 1 are similar as class 4, so are class 2 and 3. In real-world applications, when nodes in several small clusters connect to a large cluster, the surrounding differences of the nodes in the small clusters will become similar. In such case, HP filter are not able to distinguish the nodes from different small clusters.

H The Similarity, Homophily and $DD_{\hat{A}, X}(\mathcal{G})$ Metrics and Their Estimations

Additional Metrics There are three key factors that influence the performance of GNNs in real-world tasks: labels, features and graph structure. The (modified) aggregation homophily tries to investigate how the graph structure will influence the performance with labels and features being fixed. And their correlation is verified through the synthetic experiments.

Besides graph-label consistency, we need to consider feature-label consistency and aggregated-feature-label consistency as well. With aggregation similarity score of the features $S_{\text{agg}}(S(I, X))$ and aggregated features $S_{\text{agg}}(S(\hat{A}, X))$ listed in appendix H, our methods open up a new perspective on analyzing and comparing the performance of graph-agnostic models and graph-aware models in real-world tasks. Here are 2 examples.

Example 1: GCN (graph-aware model) underperforms MLP-2 (graph-agnostic model) on *Cornell*, *Wisconsin*, *Texas*, *Film*. Based on the aggregation homophily, the graph structure is not the main cause of the performance degradation. And from Table 6 we can see that the $S_{\text{agg}}(S(\hat{A}, X))$ for the above 4 datasets are lower than their corresponding $S_{\text{agg}}(S(I, X))$, which implies that it is the aggregated-feature-label inconsistency that causes the performance degradation.

Example 2: According to the widely used analysis based on node or edge homophily, the graph structure of *Chameleon*, and *Squirrel* are heterophilous and bad for GNNs. But in practice, GCN outperforms MLP-2 on those 2 datasets which means the additional graph information is helpful for node classification instead of being harmful. Traditional homophily metrics fail to explain such phenomenon but our method can give an explanation from different angles: For Chameleon, its modified aggregation homophily is not low and its $S_{\text{agg}}(S(\hat{A}, X))$ is higher than its $S_{\text{agg}}(S(I, X))$

which means its graph-label consistency and aggregated-feature-label consistency help the graph-aware model obtain the performance gain; for Squirrel, its modified aggregation homophily is low but its $S_{\text{agg}}(S(\hat{A}, X))$ is higher than its $S_{\text{agg}}(S(I, X))$ which means although its graph-label consistency is bad but the aggregated-feature-label consistency is the key factor to help the graph-aware model perform better.

We also need to point out that (modified) aggregation similarity score, $S_{\text{agg}}(S(\hat{A}, X))$ and $S_{\text{agg}}(S(I, X))$ are not deciding or threshold values because they do not consider the nonlinearity structure in the features. In practice, a low score does not tell us the GNN models will definitely perform bad.

	Cornell	Wisconsin	Texas	Film	Chameleon	Squirrel	Cora	CiteSeer	PubMed
$H_{\text{agg}}(\mathcal{G})$	0.9016	0.8884	0.847	0.8411	0.805	0.6783	0.9952	0.9913	0.9716
$S_{\text{agg}}(S(\hat{A}, X))$	0.8251	0.7769	0.6557	0.5118	0.8292	0.7216	0.9439	0.9393	0.8623
$S_{\text{agg}}(S(I, X))$	0.9672	0.8287	0.9672	0.5405	0.7931	0.701	0.9103	0.9315	0.8823
$DD_{\hat{A}, X}(\mathcal{G})$	0.3497	0.6096	0.459	0.3279	0.3109	0.2711	0.2681	0.4124	0.1889
$\hat{H}_{\text{agg}}(\mathcal{G})$	0.9046 ± 0.0282	0.9147 ± 0.0260	0.8596 ± 0.0299	0.8451 ± 0.0041	0.8041 ± 0.0078	0.6788 ± 0.0077	0.9959 ± 0.0011	0.9907 ± 0.0015	0.9724 ± 0.0015
$\hat{S}_{\text{agg}}(S(\hat{A}, X))$	0.8266 ± 0.0526	0.8280 ± 0.0351	0.6835 ± 0.0498	0.5345 ± 0.0421	0.8433 ± 0.0070	0.7352 ± 0.0132	0.9487 ± 0.0023	0.9451 ± 0.0038	0.8626 ± 0.0021
$\hat{S}_{\text{agg}}(S(I, X))$	0.9752 ± 0.0174	0.8680 ± 0.0270	0.9661 ± 0.0336	0.5438 ± 0.0184	0.8257 ± 0.0050	0.7472 ± 0.0089	0.9204 ± 0.0044	0.9441 ± 0.0036	0.8835 ± 0.0019
$\hat{D}D_{\hat{A}, X}(\mathcal{G})$	0.3936 ± 0.0663	0.6073 ± 0.0436	0.4817 ± 0.0762	0.3300 ± 0.0136	0.3329 ± 0.0151	0.3021 ± 0.0101	0.3198 ± 0.0225	0.4424 ± 0.0136	0.1919 ± 0.0046

Table 8: Additional metrics and their estimations with only training labels (mean ± std)

In most real-world applications, not all labels are available to calculate the dataset statistics. In this section, We randomly split the data into 60%/20%/20% for training/validation/test, and only use the training labels for the estimation of the statistics. We repeat each estimation for 10 times and report the mean with standard deviation. The results are shown in table 8.

Estimation The statistics we estimate are $H_{\text{agg}}(\mathcal{G})$, $S_{\text{agg}}(S(\hat{A}, X))$, $S_{\text{agg}}(S(I, X))$ and $DD_{\hat{A}, X}(\mathcal{G})$ and are denoted as $\hat{H}_{\text{agg}}(\mathcal{G})$, $\hat{S}_{\text{agg}}(S(\hat{A}, X))$, $\hat{S}_{\text{agg}}(S(I, X))$ and $\hat{D}D_{\hat{A}, X}(\mathcal{G})$. The two similarity scores $S_{\text{agg}}(S(\hat{A}, X))$ and $S_{\text{agg}}(S(I, X))$ measures the proportion of nodes, according to aggregated features and nodes features respectively, that will put larger weights on nodes in the same class than in other classes. The higher values of $S_{\text{agg}}(S(\hat{A}, X))$ and $S_{\text{agg}}(S(I, X))$ indicates the better quality of aggregated features and nodes features.

Analysis From the reported results we can see that the estimations are accurate and the errors are within the acceptable range, which means the proposed metrics and similarity scores can be accurately estimated with a subset of labels and this is important for real-world applications. Furthermore, we notice some interesting results, *e.g.*, the performance of GNNs and MLP are bad on *Squirrel* and *Film*, and according to the aggregation homophily values, the graph structure of *Film* is not quite harmful compared to other datasets, but its features and aggregated features are much worse than others; the features and aggregated features of *Squirrel* are not too bad, but its graph topology is more harmful than others. Combining the metrics defined in this paper together can help us separate different factors in graph structure and features and identify what might cause the performance degradation of GNNs.

I Experiments on Fixed Splits Provided by [33]

See table 9 for the results and table 10 the optimal searched hyperparameters.

	Cornell	Wisconsin	Texas	Film	Chameleon	Squirrel	Cora	CiteSeer	PubMed	Rank
GPRGNN	78.11 ± 6.55	82.55 ± 6.23	81.35 ± 5.32	35.16 ± 0.9	62.59 ± 2.04	46.31 ± 2.46	87.95 ± 1.18	77.13 ± 1.67	87.54 ± 0.38	8.22
H2GCN	82.70 ± 5.28	87.65 ± 4.98	84.86 ± 7.23	35.70 ± 1.00	60.11 ± 2.15	36.48 ± 1.86	87.87 ± 1.20	77.11 ± 1.57	89.49 ± 0.38	6.78
FAGCN	76.76 ± 5.87	79.61 ± 1.58	76.49 ± 2.87	34.82 ± 1.35	46.07 ± 2.11	30.83 ± 0.69	88.05 ± 1.57	77.07 ± 2.05	88.09 ± 1.38	9.56
Geom-GCN*	60.54 ± 3.67	64.51 ± 3.66	66.76 ± 2.72	31.59 ± 1.15	60.00 ± 2.81	38.15 ± 0.92	85.35 ± 1.57	78.02 ± 1.15	89.95 ± 0.47	9.22
ACM-SGC-1	82.43 ± 5.44	86.47 ± 3.77	81.89 ± 4.53	35.49 ± 1.06	63.99 ± 1.66	45.00 ± 1.4	86.9 ± 1.38	76.73 ± 1.59	88.49 ± 0.51	8.44
ACM-SGC-2	82.43 ± 5.44	86.47 ± 3.77	81.89 ± 4.53	36.04 ± 0.83	59.21 ± 2.22	40.02 ± 0.96	87.69 ± 1.07	76.59 ± 1.69	89.01 ± 0.6	8.22
ACM-GCN	85.14 ± 6.07	88.43 ± 3.22	87.84 ± 4.4	36.28 ± 1.09	66.93 ± 1.85	54.4 ± 1.88	87.91 ± 0.95	77.32 ± 1.7	90.00 ± 0.52	2.33
ACM-Snowball-2	85.41 ± 5.43	87.06 ± 2	87.57 ± 4.86	36.89 ± 1.18	67.08 ± 2.04	52.5 ± 1.49	87.42 ± 1.09	76.41 ± 1.38	89.89 ± 0.57	4.11
ACM-Snowball-3	83.24 ± 5.38	86.67 ± 4.37	87.84 ± 3.87	36.82 ± 0.94	66.91 ± 1.73	53.31 ± 1.88	87.1 ± 0.93	75.91 ± 1.57	89.81 ± 0.43	5.22
ACMII-GCN	85.95 ± 5.64	87.45 ± 3.74	86.76 ± 4.75	36.16 ± 1.11	66.91 ± 2.55	51.85 ± 1.38	88.01 ± 1.08	77.15 ± 1.45	89.89 ± 0.43	3.22
ACMII-Snowball-2	85.68 ± 5.93	87.45 ± 2.8	86.76 ± 4.43	36.55 ± 1.24	66.49 ± 1.75	50.15 ± 1.4	87.57 ± 0.86	76.92 ± 1.45	89.84 ± 0.48	4.67
ACMII-Snowball-3	82.7 ± 4.86	85.29 ± 4.23	85.41 ± 6.42	36.49 ± 1.41	66.86 ± 1.74	48.87 ± 1.23	87.16 ± 1.01	76.18 ± 1.55	89.73 ± 0.52	7.00

Table 9: Experimental results on fixed splits provided by [33]: average test accuracy \pm standard deviation on 9 real-world benchmark datasets. The best results are highlighted. Results of Geom-GCN, H₂GCN and GPRGNN are from [33, 40, 25]; results on the rest models are run by ourselves and the hyperparameter searching is the same as table 5.

J A Detailed Explanation of the Differences Between ACM(II)-GNNs and Several SOTA Models

- Difference with GPRGNN [7]: To explain the difference between channel mixing mechanism and the learning mechanism in GPRGNN, we first rewrite GPRGNN as $\mathbf{Z} = \sum_{k=0}^K \gamma_k \mathbf{H}^{(k)} = \sum_{k=0}^K \gamma_k \mathbf{I} \mathbf{H}^{(k)} = \sum_{k=0}^K \text{diag}(\gamma_k, \gamma_k, \dots, \gamma_k) \mathbf{H}^{(k)}$. The node-wise channel mixing mechanism in GPRGNN form is $\mathbf{Z} = \sum_{k=0}^K \text{diag}(\gamma_k^1, \gamma_k^2, \dots, \gamma_k^N) \mathbf{H}^{(k)}$, where N is the number of nodes and $\gamma_k^i, i = 1, \dots, N$ are learnable parametric mixing weights.
- Difference with FAGCN [4]: instead of using a fixed \hat{A} , FAGCN learns a new filter \hat{A}' based on \hat{A} . And \hat{A}' can be decomposed as $\hat{A}' = \hat{A}'_1 - \hat{A}'_2$, where \hat{A}'_1 and $-\hat{A}'_2$ represents positive and negative edge (propagation) information respectively. In our paper, we are not discussing the advantages of using the learned filter \hat{A}' over the fixed filter \hat{A} , we are comparing the models with and without channel mixing mechanism. We believe the empirical results on real-world tasks in table 2 and table 9 is the best way to compare the models with fixed filter and node-wise channel mixing and the models with learned filter but without channel mixing

Datasets	Models/Hyperparameters	lr	weight_decay	dropout	hidden	results	std	average epoch time/average total time
Cornell	ACM-SGC-1	0.01	5.00E-06	0	64	82.43	5.44	5.37ms/23.05s
	ACM-SGC-2	0.01	5.00E-06	0	64	82.43	5.44	5.93ms/25.66s
	ACM-GCN	0.05	5.00E-04	0.5	64	85.14	6.07	8.04ms/1.67s
	ACMII-GCN	0.1	1.00E-04	0	64	85.95	5.64	7.83ms/2.66s
	FAGCN	0.01	1.00E-04	0.6	64	76.76	5.87	8.80ms/7.67s
	ACM-Snowball-2	0.05	5.00E-03	0.3	64	85.41	5.43	11.50ms/2.35s
	ACM-Snowball-3	0.05	5.00E-03	0.2	64	83.24	5.38	15.06ms/3.12s
	ACMII-Snowball-2	0.1	5.00E-03	0.2	64	85.68	5.93	12.63ms/2.58s
	ACMII-Snowball-3	0.05	5.00E-03	0.2	64	82.7	4.86	14.59ms/3.06s
Wisconsin	ACM-SGC-1	0.1	5.00E-06	0	64	86.47	3.77	5.07ms/14.07s
	ACM-SGC-2	0.1	5.00E-06	0	64	86.47	3.77	5.30ms/16.05s
	ACM-GCN	0.05	1.00E-03	0.4	64	88.43	3.22	8.04ms/1.66s
	ACMII-GCN	0.01	5.00E-05	0.1	64	87.45	3.74	8.40ms/2.19s
	FAGCN	0.01	5.00E-05	0.5	64	79.61	1.59	8.61ms/5.84s
	ACM-Snowball-2	0.01	1.00E-03	0.4	64	87.06	2	12.51ms/2.60s
	ACM-Snowball-3	0.01	1.00E-02	0.1	64	86.67	4.37	14.92ms/3.15s
	ACMII-Snowball-2	0.01	5.00E-04	0.1	64	87.45	2.8	11.96ms/2.63s
	ACMII-Snowball-3	0.01	5.00E-03	0.5	64	85.29	4.23	14.87ms/3.10s
Texas	ACM-SGC-1	0.01	1.00E-05	0	64	81.89	4.53	5.34ms/19.00s
	ACM-SGC-2	0.05	1.00E-05	0	64	81.89	4.53	5.50ms/9.26s
	ACM-GCN	0.05	5.00E-04	0.5	64	87.84	4.4	9.62ms/1.99s
	ACMII-GCN	0.01	1.00E-03	0.1	64	86.76	4.75	9.98ms/2.22s
	FAGCN	0.01	1.00E-05	0	64	76.49	2.87	10.45ms/5.70s
	ACM-Snowball-2	0.01	5.00E-03	0.2	64	87.57	4.86	11.56ms/2.45s
	ACM-Snowball-3	0.01	5.00E-03	0.2	64	87.84	3.87	15.17ms/3.15s
	ACMII-Snowball-2	0.01	1.00E-03	0.2	64	86.76	4.43	11.36ms/2.30s
	ACMII-Snowball-3	0.01	5.00E-03	0.6	64	85.41	6.42	15.84ms/3.48s
Film	ACM-SGC-1	0.05	5.00E-04	0	64	35.49	1.06	5.39ms/1.17s
	ACM-SGC-2	0.05	5.00E-04	0.1	64	36.04	0.83	13.22ms/3.31s
	ACM-GCN	0.01	5.00E-03	0	64	36.28	1.09	8.96ms/1.82s
	ACMII-GCN	0.01	5.00E-03	0	64	36.16	1.11	9.06ms/1.83s
	FAGCN	0.01	5.00E-05	0.4	64	34.82	1.35	15.60ms/2.51s
	ACM-Snowball-2	0.01	1.00E-02	0	64	36.89	1.18	14.77ms/3.01s
	ACM-Snowball-3	0.01	1.00E-02	0.2	64	36.82	0.94	16.57ms/3.36s
	ACMII-Snowball-2	0.01	5.00E-03	0.1	64	36.55	1.24	12.76ms/2.57s
	ACMII-Snowball-3	0.05	5.00E-03	0.3	64	36.49	1.41	16.51ms/3.49s
Chameleon	ACM-SGC-1	0.1	5.00E-06	0.9	64	63.99	1.66	5.92ms/1.74s
	ACM-SGC-2	0.1	0.00E+00	0.9	64	59.21	2.22	8.84ms/1.78s
	ACM-GCN	0.05	5.00E-05	0.7	64	66.93	1.85	8.40ms/1.71s
	ACMII-GCN	0.05	5.00E-06	0.8	64	66.91	2.55	8.90ms/2.10s
	FAGCN	0.01	5.00E-05	0	64	46.07	2.11	16.90ms/7.94s
	ACM-Snowball-2	0.01	1.00E-04	0.7	64	67.08	2.04	12.50ms/2.69s
	ACM-Snowball-3	0.01	1.00E-05	0.8	64	66.91	1.73	16.12ms/4.91s
	ACMII-Snowball-2	0.01	5.00E-05	0.8	64	66.49	1.75	12.65ms/3.42s
	ACMII-Snowball-3	0.05	5.00E-05	0.7	64	66.86	1.74	17.60ms/4.06s
Squirrel	ACM-SGC-1	0.05	5.00E-06	0.9	64	45	1.4	6.10ms/2.18s
	ACM-SGC-2	0.05	0.00E+00	0.9	64	40.02	0.96	35.75ms/9.62s
	ACM-GCN	0.05	5.00E-06	0.7	64	54.4	1.88	10.48ms/2.68s
	ACMII-GCN	0.05	5.00E-06	0.7	64	51.85	1.38	11.69ms/2.91s
	FAGCN	0	5.00E-03	0	64	30.86	0.69	10.90ms/13.91s
	ACM-Snowball-2	0.01	1.00E-04	0.7	64	52.5	1.49	17.89ms/5.78s
	ACM-Snowball-3	0.01	5.00E-05	0.7	64	53.31	1.88	22.60ms/7.53s
	ACMII-Snowball-2	0.05	5.00E-05	0.6	64	50.15	1.4	16.95ms/3.45s
	ACMII-Snowball-3	0.01	5.00E-04	0.6	64	48.87	1.23	23.52ms/4.94s
Cora	ACM-SGC-1	0.05	5.00E-05	0.7	64	86.9	1.38	4.99ms/2.40s
	ACM-SGC-2	0.1	0	0.8	64	87.69	1.07	5.16ms/1.16s
	ACM-GCN	0.01	5.00E-05	0.6	64	87.91	0.95	8.41ms/1.84s
	ACMII-GCN	0.01	1.00E-04	0.6	64	88.01	1.08	8.59ms/1.96s
	FAGCN	0.02	1.00E-04	0.5	64	88.05	1.57	9.30ms/10.64s
	ACM-Snowball-2	0.01	1.00E-03	0.5	64	87.42	1.09	12.54ms/2.72s
	ACM-Snowball-3	0.01	5.00E-06	0.9	64	87.1	0.93	15.83ms/11.33s
	ACMII-Snowball-2	0.01	1.00E-03	0.6	64	87.57	0.86	12.06ms/2.64s
	ACMII-Snowball-3	0.01	5.00E-03	0.5	64	87.16	1.01	16.29ms/3.62s
CiteSeer	ACM-SGC-1	0.05	0.00E+00	0.7	64	76.73	1.59	5.24ms/1.14s
	ACM-SGC-2	0.1	0.00E+00	0.8	64	76.59	1.69	5.14ms/1.03s
	ACM-GCN	0.01	5.00E-06	0.3	64	77.32	1.7	8.89ms/1.79s
	ACMII-GCN	0.01	5.00E-05	0.5	64	77.15	1.45	8.95ms/1.80s
	FAGCN	0.02	5.00E-05	0.4	64	77.07	2.05	10.05ms/5.69s
	ACM-Snowball-2	0.01	5.00E-05	0	64	76.41	1.38	12.87ms/2.59s
	ACM-Snowball-3	0.01	5.00E-06	0.9	64	75.91	1.57	17.40ms/11.92s
	ACMII-Snowball-2	0.01	5.00E-03	0.5	64	76.92	1.45	13.10ms/2.94s
	ACMII-Snowball-3	0.1	5.00E-05	0.9	64	76.18	1.55	17.47ms/5.88s
PubMed	ACM-SGC-1	0.05	5.00E-06	0.4	64	88.49	0.51	5.77ms/3.65s
	ACM-SGC-2	0.05	5.00E-06	0.3	64	89.01	0.6	8.50ms/5.18s
	ACM-GCN	0.01	5.00E-05	0.4	64	90	0.52	8.99ms/2.51s
	ACMII-GCN	0.01	1.00E-04	0.3	64	89.89	0.43	9.70ms/2.57s
	FAGCN	0.01	1.00E-04	0	64	88.09	1.38	10.30ms/8.75s
	ACM-Snowball-2	0.01	1.00E-03	0.3	64	89.89	0.57	15.05ms/3.11s
	ACM-Snowball-3	0.01	5.00E-03	0.1	64	89.81	0.43	20.51ms/4.63s
	ACMII-Snowball-2	0.01	5.00E-04	0.4	64	89.84	0.48	15.10ms/3.2s
	ACMII-Snowball-3	0.01	1.00E-03	0.4	64	89.73	0.52	20.46ms/4.32s

Table 10: Hyperparameters for FAGCN and ACM-GNNs on fixed splits